Journal of Quantitative Spectroscopy & Radiative Transfer 276 (2021) 107887

Contents lists available at ScienceDirect

Journal of Quantitative Spectroscopy & Radiative Transfer

journal homepage: www.elsevier.com/locate/jqsrt

# Invariance properties of exact solutions of the radiative transfer equation

Fabrizio Martelli[a,*], Federico Tommasi[a], Lorenzo Fini[a], Lorenzo Cortese[b], Angelo Sassaroli[c], Stefano Cavalieri[a]

[a] Dipartimento di Fisica e Astronomia dell'Università degli Studi di Firenze, via Giovanni Sansone 1, 50019, Sesto Fiorentino, Firenze, Italy
[b] ICFO - Institut de Ciències Fotòniques, The Barcelona Institute of Science and Technology, 08860 Castelldefels (Barcelona), Spain
[c] Tufts University, Department of Biomedical Engineering, 4 Colby Street, Medford, Massachusetts 02155, USA

ARTICLE INFO

*Article history:*
Received 29 March 2021
Revised 6 July 2021
Accepted 13 August 2021
Available online 17 August 2021

*Keywords:*
Invariance property
Scattering media
Absorption enhancement
Disordered media
Photovoltaic
Random walk
Lambertian illumination

ABSTRACT

In this work, special invariance properties of a class of exact solutions of the radiative transfer equation (RTE) pertaining to a uniform Lambertian illumination of any non-absorbing homogeneous and inhomogeneous volume are presented and discussed. This class of solutions of the RTE traces a reference ground under which light propagation can be studied in a special simplified regime. Despite the difficulties to obtain general solutions of the radiative transfer equation, the condition of Lambertian illumination determines a unique regime of photon transport where quite easy and simple invariant solutions can be obtained in all generality for homogeneous and inhomogeneous geometries. These solutions are invariant both with respect to the geometry (size and shape of the volume) and with respect to the scattering properties, i.e. scattering coefficient, scattering function and homogeneity of the considered domain. Another evident advantage of these solutions is that they are exact solutions known with arbitrary precision and can thus be used as reference standard for photon migration studies.



## 1. Introduction

In optics, the study of light propagation may be critical when dealing with complex media and it involves many important practical applications, such as photovoltaic, biomedical applications or in optimal designing detection devices. If interference effects do not play a decisive role in the phenomenon under study, such as in the presence of scattering, an ideal and powerful framework is provided by the Radiative Transfer Equation (RTE) [1,2], whose integro-differential form, however, usually leads to solutions extremely expensive to be retrieved, both by analytical and computational approaches, also in case of simple geometries [3–13]. Despite this fact, there is an exception for which the exact solution of the RTE is very simple and easy to obtain: It is the case of a non-absorbing volume with uniform and Lambertian illumination on the external surface. From now on in this paper this kind of illumination is simply denoted as Lambertian. In this regime of propagation, the complexity of the RTE is reduced and the solution of the equation can be characterized by special invariance properties.

The aim of this paper is to provide exact invariant solutions of RTE for any non-absorbing volume with external Lambertian illumination. The importance of such solutions relies on the fact that they can be easily calculated, known with arbitrary accuracy, and proposed as a reference for analytical models or numerical simulations aimed to make predictions on radiative transport. Moreover, these solutions help the understanding of photon migration in an exemplary situation where the comprehension of propagation is simple and does not require complex mathematical approaches. Thus, these solutions may give some simple and general insights on photon migration.

The problem of a non-absorbing medium illuminated by Lambertian radiation has been recently strictly linked to a widely known invariance property for the mean total path length $\langle L \rangle$ spent by light propagating inside a disordered scattering medium [14–23]. According to such property, the mean path for a random propagation through a isotropically illuminated medium is a constant value that only depends on the geometry of the probed volume, and not on its internal disorder. Let be $V$ the volume and $\Sigma$

* Corresponding author.
*E-mail address:* fabrizio.martelli@unifi.it (F. Martelli).

https://doi.org/10.1016/j.jqsrt.2021.107887

the surface, the mean path length is:

$$\langle L\rangle = 4\frac{V}{\Sigma}. \tag{1}$$

Also known as Cauchy formula, connected to the average chord length and also used by Dirac in the context of Nuclear physics [24], the property has been revealed as an important invariant of nature. In particular, in our previous work [23] Eq. (1) has been generalized to the case where $V$ can be decomposed into $N$ scattering volumes with different refractive index, obtaining a new generalized expression:

$$\langle L\rangle = 4\frac{\sum_i^N V_i\left(\frac{n_i}{n_e}\right)^2}{\Sigma}, \tag{2}$$

where $V_i$ is the $i$th volume, $n_i$ its refractive index and $n_e$ refractive index of the external medium. In the elementary case of a single volume with refractive index mismatch with the external medium, such formula has been first introduced and used in the paper of Savo et al. [21]. This work has provided the first experimental evidence of the path length invariance property in optics. The invariance property has been studied in very different fields, leading to a complex scenario of different situations and points of view [15,19,21,23,25]. However, a complete theoretical framework able to unify the different published contributions on this subject is still missing. Our work is meant to provide a solid basis to the aforementioned invariance properties, by framing them in the context of RTE, with a further extension to all the possible solutions in presence of Lambertian illumination.

Indeed, here we show that the invariance of $\langle L\rangle$ derives from a more fundamental invariance property of the solutions for the radiance of the continuous wave (CW) RTE. Further, we show that the invariance property can be extended to more general cases, of non-scattering media and mismatched refractive index with the external environment.

In this paper, we have reviewed the CW RTE in non-absorbing media illuminated by Lambertian radiation. Solutions for the radiance, fluence rate, photon total flux and partial flux, and for the "crossing density" of photons' trajectories are obtained and their invariance properties discussed. Solutions are also provided for the special case of a non-scattering medium with a refractive index mismatch with the external medium. These solutions have been analyzed in detail providing analytical expressions for the non-scattering slab and sphere. Finally, the RTE in a non-uniform scattering medium with a non-uniform discrete distribution of refractive indices is addressed and solved for the radiance, fluence rate, photon total flux and partial flux, and for the "crossing density" of photons' trajectories through any internal surface of the medium. As special examples we have considered a layered non-scattering slab and a layered non-scattering sphere. For all the cases analyzed analytical exact solutions are provided.

In Section 2, the CW RTE for scattering volumes with uniform refractive index is introduced for the condition of Lambertian illumination and solutions are given for radiance, radiometric quantities and total mean path length. Section 3 is dedicated to the solution of the RTE for non-scattering volumes with uniform refractive index. Specific solutions are given for the geometries of slab and sphere. In Section 4, the solution of the RTE for scattering volumes with non-uniform refractive index is described. In Section 5, solutions for non-scattering volumes with non-uniform refractive index are presented with a special description provided for the non-scattering layered slab and the non-scattering layered sphere. Finally, in Section 6 the solutions obtained are discussed also by using the results of Monte Carlo (MC) simulations and emphasizing the counterintuitive aspects of the presented RTE solutions.

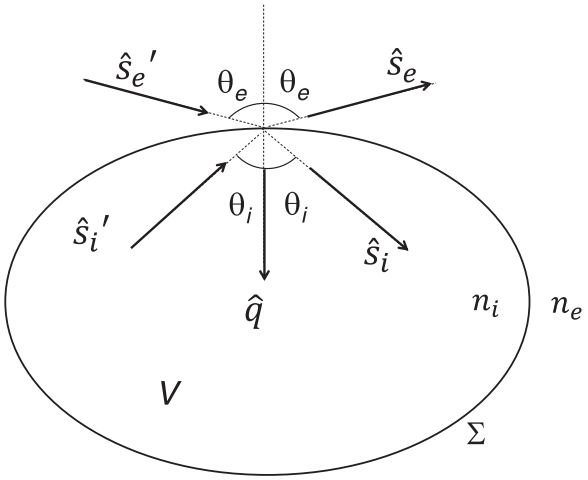


**Fig. 1.** Schematic of the main symbols used for the incidence on a volume $V$ of external surface $\Sigma$. Incidence, reflection and refraction direction vectors related by Snell's law.

## 2. RTE for scattering volumes with uniform refractive index

The geometry we consider, a non-absorbing volume without internal sources, enclosed by a smooth convex surface $\Sigma$ surrounded by a non-scattering medium, is shown in Fig. 1. The external surface is uniformly illuminated by a Lambertian CW radiation of intensity $I_0$, i.e. a uniform incident isotropic radiance distribution of light.

The source term is thus given by the following radiance distribution on $\Sigma$:

$$I_{eSource}\left(\vec{r}_\Sigma, \hat{s}_e'\right) = I_0 \ \left[\mathrm{Wm^{-2}sr^{-1}}\right] \ \forall \vec{r}_\Sigma \in \Sigma \text{ and } \forall \hat{s}_e' |\ \hat{s}_e' \cdot \hat{q} \geq 0, \tag{3}$$

thus the in-coming radiation is constant at any point on the surface and in any in-coming direction. The refractive index is $n_i$ inside the volume $V$ and $n_e$ outside. No restrictions are necessary for the scattering properties of the medium: the scattering coefficient, $\mu_s(\vec{r})$ and scattering function, $p\left(\vec{r}, \hat{s}, \hat{s}'\right)$, can thus be expressed in all generality.

The RTE for the non-absorbing volume illuminated with continuous wave radiation can be written as [1,2]:

$$\begin{aligned}\nabla \cdot \left[I\left(\vec{r}, \hat{s}\right)\hat{s}\right] + \mu_s\left(\vec{r}\right) I\left(\vec{r}, \hat{s}\right) \\ = \mu_s\left(\vec{r}\right) \int_{4\pi} p\left(\vec{r}, \hat{s}, \hat{s}'\right) I\left(\vec{r}, \hat{s}'\right) d\hat{s}' \ \ \forall \hat{s} \text{ and } \forall \ \vec{r} \in V,\end{aligned} \tag{4}$$

where $I\left(\vec{r}, \hat{s}\right)$ is the radiance inside the volume. For simplicity of notation, the direction vectors referred to the internal medium are reported without subscript.

To solve the RTE with the source term of Eq. (3) it is necessary to express the boundary conditions. About this point we assume a boundary surface with mirror reflection and refraction conditions subject to the Fresnel laws. To derive the boundary conditions we use a phenomenological approach. Specifically, at each point on the boundary surface we assume that locally, (I) the incident, reflected and transmitted fields can be approximated by plane electromagnetic waves, (II) the Fresnel laws to derive the expressions of the reflected and transmitted fields can be used, and (III) the corresponding law of energy conservation can be applied. Being the surface $\Sigma$ convex (photons leaving the medium have not the possibility to re-enter inside) and smooth (reflections only depends on the incidence angle and on the refractive index mismatch), boundary conditions are given by the:

$$\begin{aligned}I\left(\vec{r}_\Sigma, \hat{s}_i\right) = R_{ie}(\theta_i) I\left(\vec{r}_\Sigma, \hat{s}_i'\right) + T_{ei}(\theta_e)\left(\tfrac{n_i}{n_e}\right)^2 I_0 \\ \forall \vec{r}_\Sigma \in \Sigma \text{ and } \forall \hat{s}_i \,|\, 0 \leq \hat{s}_i \cdot \hat{q} \leq 1,\end{aligned} \tag{5}$$

$$I_e\left(\vec{r}_\Sigma,\hat{s}_e\right)=R_{ei}(\theta_e)I_0+T_{ie}(\theta_i)\left(\tfrac{n_e}{n_i}\right)^2 I\left(\vec{r}_\Sigma,\hat{s}_i'\right)$$
$$\forall\vec{r}_\Sigma\in\Sigma\text{ and }\forall\hat{s}_e\,|\,-1\le\hat{s}_e\cdot\hat{q}\le 0, \tag{6}$$

where: the unitary directions vectors $\hat{s}_i$, $\hat{s}_i'$, $\hat{s}_e$ and $\hat{q}$ are related by Snell's laws; $R_{ie}$ and $T_{ie}$, $R_{ei}$ and $T_{ei}$ are the Fresnel reflection and transmission coefficients for unpolarized light respectively, from internal to external (ie) and viceversa (ei) [2]; $I\left(\vec{r}_\Sigma,\hat{s}_i\right)$ is the inwardly directed radiance on the boundary, and $I_e\left(\vec{r}_\Sigma,\hat{s}_e\right)$ the outwardly directed radiance on the boundary, i.e., the outgoing radiance.

Equation (5) states that the power flowing in the internal medium $i$ in the incoming directions $\hat{s}_i$ per unit surface is equal to the sum of (I) the fraction of the power transmitted from the external $e$ to the internal $i$ medium per unit surface around the in-coming direction $\hat{s}_e'$ and (II) the fraction of the power reflected in the internal medium per unit surface around the out-coming direction $\hat{s}_i'$, where for any specified direction $\hat{s}_i$, $\hat{s}_i'$ is the mirror direction of $\hat{s}_i$ with respect to $\Sigma$.

Equation (6) states that the power flowing in the external medium $e$ in the outcoming directions $\hat{s}_e$ per unit surface is equal to the sum of (I) the fraction of the power transmitted from the internal $i$ to the external $e$ medium per unit surface around the out-coming direction $\hat{s}_i'$ and (II) the fraction of the power reflected in the external medium per unit surface around the in-coming directions $\hat{s}_e'$, where for any specified direction $\hat{s}_e$, $\hat{s}_e'$ is the mirror direction of $\hat{s}_e$ with respect to $\Sigma$.

The coefficients $\left(\frac{n_i}{n_e}\right)^2$ and $\left(\frac{n_e}{n_i}\right)^2$ account for the different geometrical extent of the light beam element at the boundary $\Sigma$ due to refraction when passing from the external (e) to the internal (i) medium and viceversa. Being $T_{ei}(\theta_e)=1-R_{ei}(\theta_e)$, $T_{ie}(\theta_i)=1-R_{ie}(\theta_i)$, and also $T_{ei}(\theta_e)=T_{ie}(\theta_i)$ with $\theta_i$ and $\theta_e$ related by Snell's law, Eqs. (5) and (6) can thus be rewritten as:

$$I\left(\vec{r}_\Sigma,\hat{s}_i\right)=R_{ie}(\theta_i)I\left(\vec{r}_\Sigma,\hat{s}_i'\right)+(1-R_{ie}(\theta_i))\left(\tfrac{n_i}{n_e}\right)^2 I_0$$
$$\forall\vec{r}_\Sigma\in\Sigma\text{ and }\forall\hat{s}_i\,|\,0\le\hat{s}_i\cdot\hat{q}\le 1, \tag{7}$$

$$I_e\left(\vec{r}_\Sigma,\hat{s}_e\right)=R_{ei}(\theta_e)I_0+(1-R_{ei}(\theta_e))\left(\tfrac{n_e}{n_i}\right)^2 I\left(\vec{r}_\Sigma,\hat{s}_i'\right)$$
$$\forall\vec{r}_\Sigma\in\Sigma\text{ and }\forall\hat{s}_e\,|\,-1\le\hat{s}_e\cdot\hat{q}\le 0. \tag{8}$$

All the solutions that will be obtained in the next sections exploit the hypothesis of convex volume. This fact is related to the kind of illumination of the volume used, i.e. a source distributed on the external surface (Eq. (4)). Indeed, by selecting an external suitable illumination impinging over the external surface of the volume, it would be possible to have RTE solutions for no-convex volumes. In this case it would be also possible to release the hypothesis of non-scattering external medium. However, we have chosen the source distributed on the external surface as Eq. (4) since this approach allows an easier and well defined treatment of the boundary conditions, accordingly to Eqs. (7) and (8).

### 2.1. Solutions for radiance and other radiometric quantities

The solution of the RTE for the radiance, that also fulfills the boundary conditions of Eqs. (7) and (8), is:

$$I\left(\vec{r},\hat{s}\right)=\left(\tfrac{n_i}{n_e}\right)^2 I_0\ \left[\mathrm{Wm^{-2}sr^{-1}}\right]\ \forall\hat{s}\text{ and }\ \forall\vec{r}\in V, \tag{9}$$

$$I_e\left(\vec{r}_\Sigma,\hat{s}\right)=I_0\ \left[\mathrm{Wm^{-2}sr^{-1}}\right]$$
$$\forall\vec{r}_\Sigma\in\Sigma\text{ and }\forall\hat{s}\,|\,-1\le\hat{s}\cdot\hat{q}\le 0, \tag{10}$$

where $I\left(\vec{r},\hat{s}\right)$ is the internal radiance and $I_e\left(\vec{r}_\Sigma,\hat{s}\right)$ the radiance outgoing the surface $\Sigma$. The simple substitution of the above equations into Eq. (4) proves that they are the RTE solutions with the given boundary conditions. The first term of RTE vanishes since it is applied to a constant term. The other two terms cancel out due to the normalization condition of the phase function. Moreover, these solutions are unique due to the fact that they are RTE solutions that fulfill the given boundary conditions for the radiance on the whole external boundary of the medium for any direction [26]. It is worth to point out that for the CW RTE the stationary distribution of radiance inside the considered volume, given its geometry and optical properties, is uniquely determined by the sources in the volume and by the incident radiance distribution [26]. In this specific case, since we have only external sources, the uniqueness is guaranteed by the incident Lambertian radiance distribution requested with Eqs. (5) and (6).

The internal radiance $I$ is thus uniform and isotropic and its value is only determined by the incident radiance $I_0$ and by the refractive index mismatch between internal and external medium. Also the re-emitted radiation, $I_e$, is uniform and Lambertian (i.e. with isotropic distribution) and with intensity identical to the incoming radiance. We point out that both the solution for the outgoing radiance, $I_e\left(\vec{r}_\Sigma,\hat{s}\right)$, and the solution for the internal radiance, $I\left(\vec{r},\hat{s}\right)$, are invariant both with respect to the geometry (size and shape of the volume, provided the external surface is convex and flat) and with respect to the scattering properties (scattering coefficient, scattering function, homogeneity). These solutions can therefore be used in all generality with only one exception: the case of non-scattering volume with $n_i>n_e$. In this case (see Section 3) the solution for $I\left(\vec{r},\hat{s}\right)$ may depend on the shape of the volume.

Making use of the above solution simple expressions are also obtained for other radiometric quantities. For the fluence rate, $\Phi(\vec{r})$, and the total photon flux, $\vec{J}(\vec{r})$, inside the medium we have:

$$\Phi(\vec{r})=\int_{4\pi} I\left(\vec{r},\hat{s}\right)d\hat{s}=4\pi\left(\tfrac{n_i}{n_e}\right)^2 I_0\ \ \left[\mathrm{Wm^{-2}}\right], \tag{11}$$

$$\vec{J}(\vec{r})=\int_{4\pi} I\left(\vec{r},\hat{s}\right)\hat{s}d\hat{s}=0\ \ \left[\mathrm{Wm^{-2}}\right]. \tag{12}$$

Equation (12) states that the net total flux through whatever surface element inside the medium must be null. This means that the number of photons crossing any internal surface in a specific direction must be identical to the number of crossing in the opposite one.

It may be also interesting to evaluate the normal component of the partial flux within the semi-solid angle, since it characterizes the passage through a surface element of photons from one side to another. In particular, the component of the partial flux on the external surface $\Sigma$ along the inward normal direction $\hat{q}$, i.e., the incident flux $J_{e+}$, is obtained integrating over the inward semi-solid angle:

$$J_{e+}(\vec{r})=\int_{\hat{s}\cdot\hat{q}\ge 0} I_{eSource}\left(\vec{r},\hat{s}\right)\hat{s}\cdot\hat{q}d\hat{s}=$$
$$=2\pi I_0\int_0^{\pi/2}\cos\theta\sin\theta d\theta=\pi I_0\ \left[\mathrm{Wm^{-2}}\right]\ \forall\vec{r}\in\Sigma. \tag{13}$$

Similarly for the outgoing flux, $J_{e-}(\vec{r})$, from $\Sigma$:

$$J_{e-}(\vec{r})=\int_{\hat{s}\cdot\hat{q}\le 0} I_e\left(\vec{r},\hat{s}\right)\hat{s}\cdot\hat{q}d\hat{s}=-\pi I_0\ \left[\mathrm{Wm^{-2}}\right]\ \forall\vec{r}\in\Sigma, \tag{14}$$

for which we obviously (the medium is non-absorbing) have $J_{e+}(\vec{r})=-J_{e-}(\vec{r})$. These components of the flux provide information on the number of photons crossing the surface element in a specific direction and thus are related to the photons' trajectory density. From Eq. (13) we also have that the total incident power, $P_{e+Tot}(\vec{r})$, is

$$P_{e+Tot}(\vec{r})=\pi I_0\Sigma. \tag{15}$$

Similarly, the components of the partial flux across an internal surface element, i.e., a surface element internal to $V$, are

$$J_{+}(\vec{r})=\int_{\hat{s}\cdot\hat{q}\ge 0} I\left(\vec{r},\hat{s}\right)\hat{s}\cdot\hat{q}d\hat{s}=\pi\left(\tfrac{n_i}{n_e}\right)^2 I_0\ \left[\mathrm{Wm^{-2}}\right]\ \forall\vec{r}\in V, \tag{16}$$

$$J_{-}(\vec{r})=\int_{\hat{s}\cdot\hat{q}\le 0} I\left(\vec{r},\hat{s}\right)\hat{s}\cdot\hat{q}d\hat{s}=-\pi\left(\tfrac{n_i}{n_e}\right)^2 I_0\ \left[\mathrm{Wm^{-2}}\right]\ \forall\vec{r}\in V, \tag{17}$$

where $\hat{q}$ is the unit vector normal to the surface element. Also for the components of the internal flux is $J_+(\vec{r}) = -J_-(\vec{r})$.

It is worth to note that, if we use the energy of a photon as the unit for energy, the partial flux can be viewed as proportional to the number of photons crossing the unit surface per unit time: flux $J_+$ ($J_-$) increases (decreases) of one unit each time a trajectory crosses the surface with $\hat{s}\cdot\hat{q} \geq 0$ ($\hat{s}\cdot\hat{q} \leq 0$). Therefore, photons crossing several times the surface give multiple contributions to the flux, while photons that never cross the surface give a null contribution.

Therefore, $J_+$ and $J_-$ are proportional to the number of times photons cross the surface in a direction, $N_{cross+}$, or in the opposite one, $N_{cross-}$. In other words, $J_+$ and $J_-$ can be considered as an internal "trajectory density" or "crossing density", i.e. proportional to the number of crossing photons.

In a similar way, $J_{e+}$, can be considered as the "trajectory density" or "crossing density" for emitted photons.

It can be also defined the total number of crossing photons $N_{cross} = N_{cross+} + N_{cross-}$. By using the above Eqs. (13), (16) and (17) we have that the internal "trajectory density" or "crossing density", $\rho_{Ncross}$, number of crossing photons per unit of emitted photons is:

$$\rho_{Ncross} = \frac{N_{cross}}{N_{e+}} = \frac{N_{cross+}+N_{cross-}}{N_{e+}} = \frac{J_+ + |J_-|}{J_{e+}} = \frac{2J_+}{J_{e+}} = 2\left(\frac{n_i}{n_e}\right)^2. \tag{18}$$

Wherever the internal surface element is, and whatever the scattering properties are (apart the case $\mu_s(\vec{r}) = 0$, see Section 3), the internal "trajectory density" or "crossing density" only depends on the refractive index mismatch between medium and external environment.

As easily predictable the invariance property observed for the solution of the RTE also applies to the other radiometric quantities: Also the solutions shown for fluence, flux, partial flux, etc are independent of both the geometry and the scattering properties of the volume.

### 2.2. Solution for average internal path length

The solution of the RTE obtained for the fluence rate, Eq. (11), allows us to calculate the average internal length of trajectories followed by photons inside a non-absorbing volume with the external surface illuminated with CW Lambertian radiation. The value for the average total path length is obtained by calculating the total absorbed radiation in the limit of zero absorption in two different ways. The first way is to integrate the local absorption, $\mu_a(\vec{r}_V)\Phi(\vec{r}_V)d\vec{r}_V$, over the volume $V$ of the medium:

$$P_{A1} = \int_V \mu_a(\vec{r}_V)\Phi(\vec{r}_V)d\vec{r}_V, \tag{19}$$

that for uniform absorption and in the limit of zero absorption becomes:

$$\lim_{\mu_a\to 0} P_{A1} = \lim_{\mu_a\to 0}\int_V \mu_a(\vec{r}_V)\Phi(\vec{r}_V)d\vec{r}_V = \lim_{\mu_a\to 0} 4\pi\,\mu_a\left(\frac{n_i}{n_e}\right)^2 I_0 V, \tag{20}$$

where we have used Eq. (11), i.e., the fluence for the non-absorbing medium.

The second way to calculate the total absorbed power in $V$ involves the probability density function for the photons' path length and the microscopic Lambert-Beer law [2,27]. For photons travelling a trajectory of total length $L$ through a volume with uniform absorption, the probability that absorption occurs is $[1-\exp(-\mu_a L)]$ [2,27]. If $p(L,\mu_a=0)$ is the probability density function that photons follow a trajectory of length $L$ for the non-absorbing medium, and $P_I$ the total incident power, then the total absorbed power can be calculated as:

$$P_{A2} = P_I\int_0^\infty p(L,\mu_a=0)[1-\exp(-\mu_a L)]dL, \tag{21}$$

and in the limit of zero absorption:

$$\lim_{\mu_a\to 0} P_{A2} = P_I\int_0^\infty \mu_a L p(L,\mu_a=0)dL = P_I\mu_a\langle L\rangle(\mu_a=0). \tag{22}$$

We point out that the probability density function $p(L,\mu_a=0)$ pertains to the totality of the incident radiation. Therefore, $p(L,\mu_a=0)$, when the refractive index of the medium $n_i$ is different from the refractive index of the external medium $n_e$, will also include a term $R_{TotLamb}\,\delta(L)$ (with $R_{TotLamb}$ total reflection coefficient for Lambertian incidence and $\delta(L)$ Dirac delta function of $L$) which takes into account radiation reflected on the external surface $\Sigma$. It is important to note that part of the incident radiation reflected at the boundary, when present, gives a fundamental contribution to the RTE solutions and to the related invariance properties.

According to Eq. (15), the total incident power is $P_I = \pi I_0 \Sigma$. Thus, by equaling $P_{A1}$ and $P_{A2}$ in the limit $\mu_a \to 0$, it is possible to express $\langle L\rangle(\mu_a=0)$ as:

$$\langle L\rangle(\mu_a=0) = 4\left(\frac{n_i}{n_e}\right)^2\frac{V}{\Sigma} = \Phi(\vec{r},\mu_a=0)\frac{V}{\pi\Sigma I_0}\quad [\mathrm{m}]. \tag{23}$$

Equation (23) shows that the average path length $\langle L\rangle$ for the non-absorbing medium depends on the refractive index mismatch and on the ratio between the volume of the medium and its external surface area, but it is invariant with respect the scattering properties (apart for $\mu_s(\vec{r}) = 0$). Such invariance property is a generalization of the mean chord length theorem, valid for ballistic propagation and also used in the context of nuclear physics [14,26]. Therefore, among the invariance properties observed for the radiance and other radiometric quantities (invariance with respect to the geometry, and invariance with respect to the scattering properties) only the invariance with respect to the scattering properties also applies to the average path length $\langle L\rangle(\mu_a=0)$. Anyway, the dependence on the geometry of the illuminated medium is very simple and only involves the ratio $\frac{V}{\Sigma}$.

For the infinitely extended slab of thickness $s_0$, Eq. (23) becomes:

$$\langle L\rangle_{Slab}(\mu_a=0) = 2s_0\left(\frac{n_i}{n_e}\right)^2, \tag{24}$$

for the sphere of radius $R_0$:

$$\langle L\rangle_{Sphere}(\mu_a=0) = \tfrac{4}{3}R_0\left(\frac{n_i}{n_e}\right)^2, \tag{25}$$

and for the infinite cylinder with radius $R_0$:

$$\langle L\rangle_{Cylinder}(\mu_a=0) = 2R_0\left(\frac{n_i}{n_e}\right)^2. \tag{26}$$

## 3. RTE for non-scattering volumes with uniform refractive index

For non-scattering and non-absorbing volumes the RTE (Eq. (4)) reduces to

$$\nabla\cdot[I(\vec{r},\hat{s})\hat{s}] = 0\ \ \forall\hat{s}\ \text{and}\ \ \forall\vec{r}\in V, \tag{27}$$

that can also be written as:

$$\frac{\partial I(\vec{r},\hat{s})}{\partial s} = 0\ \ \forall\hat{s}\ \text{and}\ \ \forall\vec{r}\in V. \tag{28}$$

These equations state that the radiance does not change inside the volume $V$ along a fixed direction $\hat{s}$.

Light propagation is thus determined only by the boundary conditions, i.e. by Eqs. (7) and (8).

Solutions for non-scattering volumes are described separately for $n_i \leq n_e$ and $n_i > n_e$.

### 3.1. Solution for $n_i \leq n_e$

When $n_i \leq n_e$, it is $R_{ie}(\theta_i) < 1$ for any angle $\theta_i < \pi/2$ and the boundary conditions of Eqs. (7) and (8) in this case are fulfilled by the following solutions:

$$\begin{aligned} &I(\vec{r},\hat{s}) = \left(\frac{n_i}{n_e}\right)^2 I_0\ \ \forall\hat{s}\ \text{and}\ \ \forall\vec{r}\in V\\ &I_e(\vec{r}_\Sigma,\hat{s}) = I_0\ \forall\vec{r}_\Sigma\in\Sigma\ \text{and}\ \forall\hat{s}\,|\,-1\leq\hat{s}\cdot\hat{q}\leq 0. \end{aligned} \tag{29}$$

Thus, for $n_i \le n_e$ the solutions for the radiance are identical to those for $\mu_s(\vec{r}) \neq 0$ (Eqs. (9) and (10)), with an internal radiance uniform and isotropic. Also the solutions for fluence rate, mean path length, etc. will be identical to those for scattering volumes described in Sections 2.1 and 2.2.

### 3.2. Solution for $n_i > n_e$

When $n_i > n_e$, it is $R_{ie}(\theta_i) = 1$ for $\theta_i \ge \theta_{cie}$, with $\sin\theta_{cie} = n_e/n_i$ and the boundary conditions can be re-written as:

$$I\left(\vec{r}_\Sigma, \hat{s}_i\right) = R_{ie}(\theta_i) I\left(\vec{r}, \hat{s}_i'\right) + [1 - R_{ie}(\theta_i)]\left(\tfrac{n_i}{n_e}\right)^2 I_0 \quad \forall \vec{r}_\Sigma \in \Sigma, \text{ and } \forall \hat{s}_i \mid \cos\theta_{cie} \le \hat{s}_i \cdot \hat{q} \le 1, \text{ i.e. } \theta_i < \theta_{cie} \tag{30}$$

$$I\left(\vec{r}_\Sigma, \hat{s}_i\right) = I\left(\vec{r}_\Sigma, \hat{s}_i'\right) \quad \forall \vec{r}_\Sigma \in \Sigma, \ \forall \hat{s}_i \mid 0 \le \hat{s}_i \cdot \hat{q} \le \cos\theta_{cie}, \text{ i.e. } \theta_i \ge \theta_{cie} \tag{31}$$

$$I_e\left(\vec{r}_\Sigma, \hat{s}_e\right) = R_{ei}(\theta_e) I_0 + (1 - R_{ei}(\theta_e))\left(\tfrac{n_e}{n_i}\right)^2 I\left(\vec{r}_\Sigma, \hat{s}_i'\right) \quad \forall \vec{r}_\Sigma \in \Sigma \text{ and } \forall \hat{s}_e \mid -1 \le \hat{s}_e \cdot \hat{q} \le 0, \tag{32}$$

where Eq. (7) has been split for $\theta_i < \theta_{cie}$ and for $\theta_i \ge \theta_{cie}$.

Equations (30) and (32) determine the same RTE solutions found for scattering media but only at the boundary points, $\vec{r}_\Sigma$, and for angles $\theta_i < \theta_{cie}$. Thus, we obtain for the radiance on the internal surface:

$$I\left(\vec{r}_\Sigma, \hat{s}_i\right) = \left(\tfrac{n_i}{n_e}\right)^2 I_0 \quad \forall \vec{r}_\Sigma \in \Sigma, \ \forall \hat{s}_i \mid \cos\theta_{cie} \le \hat{s}_i \cdot \hat{q} \le 1, \text{ i.e. } \theta_i < \theta_{cie}. \tag{33}$$

Similarly, from Eqs. (6) and (29), for the radiance on the external surface the solution is

$$I_e\left(\vec{r}_\Sigma, \hat{s}_e\right) = I_0 \quad \forall \vec{r}_\Sigma \in \Sigma, \text{ and } \forall \hat{s}_e \mid -1 \le \hat{s}_e \cdot \hat{q} \le 0. \tag{34}$$

The solutions for the radiance on the internal surface for angles $\theta_i < \theta_{cie}$, and for the external radiance are identical to those for the volume with $\mu_s(\vec{r}) \neq 0$ (Eqs. (9) and (10)).

However, it must be noted that for angles $\theta_i \ge \theta_{cie}$, Eq. (31) is not sufficient to obtain a general univocal solution for the radiance on the internal surface. Therefore, also the solution for the radiance $I\left(\vec{r}, \hat{s}\right)$ within the volume remains undetermined: a solution can be found only with detailed information on the shape of the external surface $\Sigma$. Indeed, the solution is still unique, accordingly to the general theorem of Ref. [26], however the RTE solution for angles $\theta_i > \theta_{cie}$ depends on the geometry considered, i.e. on the external surface $\Sigma$. Thus, detailed characteristics of the geometry have to be considered. As long as the geometry of the medium is not known, it is not possible to determine the unique solution for angles $\theta_i > \theta_{cie}$ that in general may be different from the solution for $\theta_i < \theta_{cie}$.

As a general outcome, multiple internal reflections tend to randomize directions of propagation and to reestablish the homogeneity and isotropy of internal radiance also for $n_i > n_e$. In this case, solutions for $I\left(\vec{r}, \hat{s}\right)$, $\Phi(\vec{r})$, $\vec{J}(\vec{r})$, $J_{e+}(\vec{r})$, $J_+(\vec{r})$, $J_-(\vec{r})$, $\rho_{Ncross}$ and $\langle L \rangle$ are identical to those for the scattering volume and also the invariance property for the average path length holds. However, for nonergodic geometries this does not fully happen as for instance in the plane-parallel slab and in the sphere. As noted by Yablonovitch [28] nonergodic geometries are “unusual and exceptional” and “the symmetry is so high that only a restricted class of angles is dynamically accessible to an incoming light ray”. Moreover, whispering gallery modes does exist in any smooth convex domain as shown by Lazutkin [29]. These facts imply that for $n_i > n_e$ there are geometries with high-symmetry for which multiple internal reflections do not reproduce the solutions for the radiance found for $n_i < n_e$.

Thus, for geometries like slab and sphere, due to particular symmetries, for $n_i > n_e$ there are conditions for internal guided propagation, i.e. trapped ray trajectories. Thus, isotropic and/or uniform radiance inside the medium cannot be established, because the internal incidence angle remains the same for all reflection orders. In these cases solutions must be determined case-by-case. In the next section, we discuss the solutions for slab and sphere.

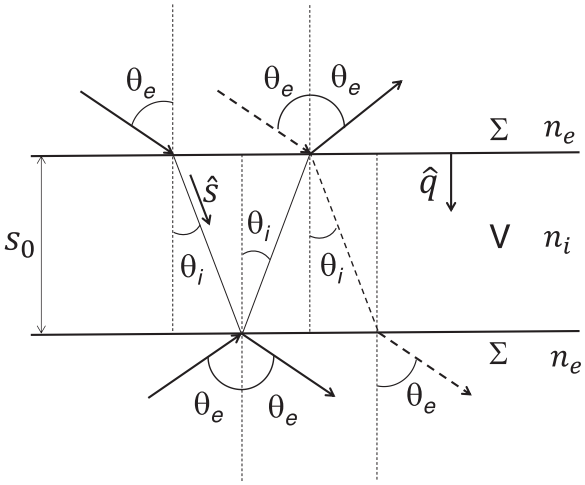


**Fig. 2.** Refraction and reflection in the laterally infinitely extended slab. $\hat{q}$ is the unitary vector normal to the sides of the slab inwardly directed.

#### 3.2.1. Slab geometry

Since the solutions for non-scattering volumes with $n_i \le n_e$ are identical to those for scattering volumes, we consider here only the case $n_i > n_e$. Let's consider a non-absorbing slab of thickness $s_0$ and refractive index $n_i$ (see Fig. 2). For a non-scattering laterally infinitely extended slab, the trajectories of photons entering along the same direction, during propagation always remain parallel to each other anywhere they enter. The internal radiance will be therefore identical to the radiance on the internal boundary. From Eq. (33) we therefore have for angles smaller than the critical angle $\theta_{cie}$ ($\sin\theta_{cie} = \frac{n_e}{n_i}$) that:

$$I\left(\vec{r}, \hat{s}\right) = \left(\tfrac{n_i}{n_e}\right)^2 I_0 \quad \forall \vec{r} \in V, \ \forall \hat{s} \mid \cos(\theta_{cie}) \le |\hat{s} \cdot \hat{q}| \le 1, \tag{35}$$

whereas for angles greater than $\theta_{cie}$ we have:

$$I\left(\vec{r}, \hat{s}\right) = 0 \quad \forall \vec{r} \in V, \ \forall \hat{s} \mid |\hat{s} \cdot \hat{q}| < \cos\theta_{cie}, \ \theta_{cie} < \theta_i < \pi - \theta_{cie} \tag{36}$$

since no photons can arise inside the slab with angles greater than the critical angle. Therefore there is an angular discontinuity of radiance inside the slab. Equations (35) and (36) provide the full description of the internal radiance from which solutions for fluence, flux, etc, can be easily obtained. Consequently, it results:

$$\Phi(\vec{r}) = 2\pi 2 \int_0^{\theta_{cie}} \left(\tfrac{n_i}{n_e}\right)^2 I_0 \sin\theta d\theta = 4\pi \left(\tfrac{n_i}{n_e}\right)^2 I_0 \left[1 - \sqrt{1 - \left(\tfrac{n_e}{n_i}\right)^2}\right], \tag{37}$$

$$\vec{J}(\vec{r}) = \int_{4\pi} I\left(\vec{r}, \hat{s}\right) \hat{s} d\hat{s} = 0, \tag{38}$$

$$J_{e+}(\vec{r}) = \int_{\hat{s}\cdot\hat{q}\ge 0} I_{eSource}\left(\vec{r}, \hat{s}\right) \hat{s} \cdot \hat{q} d\hat{s} = \pi I_0, \tag{39}$$

$$J_+(\vec{r}) = -J_-(\vec{r}) = 2\pi \int_0^{\theta_{cie}} \left(\tfrac{n_i}{n_e}\right)^2 I_0 \cos\theta \sin\theta d\theta = \pi \left(\tfrac{n_i}{n_e}\right)^2 I_0 \left(\tfrac{n_e}{n_i}\right)^2 = \pi I_0, \tag{40}$$

$$\rho_{Ncross} = \frac{N_{cross}}{N_{e+}} = \frac{2J_+}{J_{e+}} = 2. \tag{41}$$

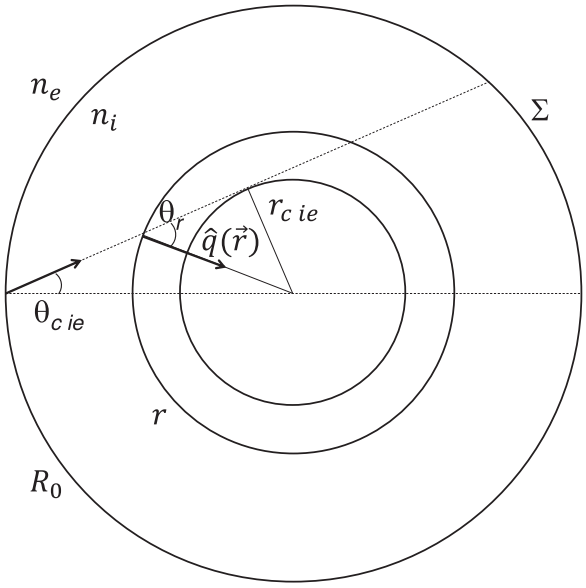


**Fig. 3.** Schematic for non-scattering sphere: internal-external critical angle. The symbol $r$ denotes $|\vec{r}|$.

The factor 2 in Eq. (37) takes into account the incident radiance from both sides of the slab. Since the internal fluence is uniform, the internal average path length can be obtained in a simple way following the procedure used in Section 2.2. Using in Eq. (20) the fluence given by Eq. (37), and then by acting as in Section 2.2 we obtain for the average path length $\langle L\rangle$:

$$\langle L\rangle = 2s_0\left(\frac{n_i}{n_e}\right)^2\left[1-\sqrt{1-\left(\frac{n_e}{n_i}\right)^2}\right]. \tag{42}$$

If we compare this equation with Eq. (24), we realize that $\langle L\rangle$ is discontinuous with the scattering properties in the case of guided propagation. For any arbitrarily small scattering value, Eq. (24) holds, while Eq. (42) holds for $\mu_s = 0$. The same result has been also obtained by Majic et al. [30] by following two different approaches for the scattering (thermodynamic) and nonscattering (ray optics) cases.

Solutions for the non-scattering slab with $n_i > n_e$ are therefore significantly different from those for the scattering slab. In particular, the internal radiance $I(\vec{r},\hat{s})$ is independent of $\vec{r}$ but non-isotropic. The fluence is uniform, however its value differs from the value for the scattering slab and we have thus a discontinuity between the solution with and without scattering. Also the internal partial flux component along the normal direction $\hat{q}$ does not reproduce the value for the scattering slab and its value is $J_+(\vec{r}) = J_{e+}(\vec{r})$.

Finally, also the solution for the average path length $\langle L\rangle$ is different from that obtained for the scattering slab (Eq. (24)) because of the internal-external critical angle. Therefore, the invariance property as was presented for the scattering slab does not apply for the non-scattering slab with $n_i > n_e$.

In Appendix, we have shown how solutions for the non-scattering slab can also be obtained following a different approach only based on Snell's and Fresnel's laws. The two procedures obviously return the same solutions.

### 3.2.2. Sphere geometry

Let's consider a sphere of radius $R_0$ with refractive index $n_i$ (see Fig. 3). When $n_i > n_e$, the internal radiance for a non-scattering and non-absorbing sphere with Lambertian surface illumination is obtained from the radiance on the internal boundary. Indeed, in absence of scattering, the radiance at the internal boundary fully determines the radiance in the inner part of the sphere. In this calculation it must be accounted for the contributions from all the boundary $\Sigma$. From Eqs. (30) and (31), taking into account that the internal incidence angle remains unchanged regardless of the number of internal reflections that may occur at the internal boundary of the sphere, the radiance on the internal boundary results:

$$\begin{aligned} &I(\vec{r}_\Sigma,\hat{s}) = \left(\tfrac{n_i}{n_e}\right)^2 I_0 \\ &\forall\vec{r}_\Sigma\in\Sigma,\ \forall\hat{s}\,|\,\cos\theta_{cie} < \hat{s}\cdot\hat{q} \le 1,\ \text{i.e.}\,\theta_i < \theta_{cie} \\ &I(\vec{r}_\Sigma,\hat{s}) = 0 \\ &\forall\vec{r}_\Sigma\in\Sigma,\ \forall\hat{s}\,|\,|\hat{s}\cdot\hat{q}| < \cos\theta_{cie},\ \text{i.e.}\,\theta_i > \theta_{cie}, \end{aligned} \tag{43}$$

where $\hat{q}$ is the normal inwardly directed and $\sin\theta_{cie} = \frac{n_e}{n_i}$.

Making reference to Fig. 3, the internal radiance can be written as:

$$\begin{aligned} &I(\vec{r},\hat{s}) = \left(\tfrac{n_i}{n_e}\right)^2 I_0\ \ \forall\vec{r}\,|\,r\le r_{cie},\ \forall\hat{s}\,|\,-1<\hat{s}\cdot\hat{q}(\vec{r})\le 1 \\ &I(\vec{r},\hat{s}) = \left(\tfrac{n_i}{n_e}\right)^2 I_0\ \ \forall\vec{r}\,|\,r> r_{cie},\ \forall\hat{s}\,|\,\arccos\left[|\hat{s}\cdot\hat{q}(\vec{r})|\right]\le\theta(r) \\ &I(\vec{r},\hat{s}) = 0\ \ \forall\vec{r}\,|\,r> r_{cie},\ \forall\hat{s}\,|\,\arccos\left[|\hat{s}\cdot\hat{q}(\vec{r})|\right]>\theta(r), \end{aligned} \tag{44}$$

where $\hat{q}(\vec{r})$ is the inwardly directed normal to the sphere with radius $r$, $r_{cie} = R_0\sin\theta_{cie} = R_0\frac{n_e}{n_i}$, $\theta(r) = \arcsin\left[\frac{r_{cie}}{r}\right]$, and $R_0$ is the radius of the sphere. From the above internal distribution of radiance it is possible to calculate the internal fluence rate as:

$$\begin{aligned} &\Phi(\vec{r}) = 2\pi\int_0^{\pi}\left(\tfrac{n_i}{n_e}\right)^2 I_0\sin\theta d\theta = 4\pi\left(\tfrac{n_i}{n_e}\right)^2 I_0,\ \ \forall r\le r_{cie} \\ &\Phi(\vec{r}) = 2\pi 2\int_0^{\theta(r)}\left(\tfrac{n_i}{n_e}\right)^2 I_0\sin\theta d\theta = \\ &= 4\pi\left(\tfrac{n_i}{n_e}\right)^2 I_0\left[1-\sqrt{1-\left(\tfrac{r_{cie}}{r}\right)^2}\right],\ \ \forall r> r_{cie}. \end{aligned} \tag{45}$$

For the total flux we have:

$$\vec{J}(\vec{r}) = \int_{4\pi} I(\vec{r},\hat{s})\hat{s}d\hat{s} = 0, \tag{46}$$

and the components of the partial flux along the radial direction $\hat{q}$ are:

$$J_{e+}(\vec{r}) = \int_{\hat{s}\cdot\hat{q}\ge 1} I_{esource}(\vec{r},\hat{s})\hat{s}\cdot\hat{q}(r)d\hat{s} = \pi I_0,\ \ \forall\vec{r}\in\Sigma, \tag{47}$$

$$\begin{aligned} &J_+(\vec{r}) = -J_-(\vec{r}) = 2\pi\int_0^{\pi/2}\left(\tfrac{n_i}{n_e}\right)^2 I_0\hat{s}\cdot\hat{q}(r)\sin\theta d\theta = \\ &= \pi\left(\tfrac{n_i}{n_e}\right)^2 I_0,\ \ \forall r\le r_{cie} \\ &J_+(\vec{r}) = -J_-(\vec{r}) = 2\pi\int_0^{\theta(r)}\left(\tfrac{n_i}{n_e}\right)^2 I_0\hat{s}\cdot\hat{q}(r)\sin\theta d\theta = \\ &= \pi\left(\tfrac{n_i}{n_e}\right)^2 I_0\left[\tfrac{R_0}{r}\tfrac{n_e}{n_1}\right]^2 = \pi\left(\tfrac{R_0}{r}\right)^2 I_0,\ \ \forall r> r_{cie}. \end{aligned} \tag{48}$$

Finally, we can write the solution for the "trajectory density" or "crossing density":

$$\begin{aligned} &\rho_{Ncross} = \tfrac{N_{cross}}{N_{e+}} = \tfrac{2J_+}{J_{e+}} = 2\left(\tfrac{n_i}{n_e}\right)^2\ \ \forall r\le r_{cie} \\ &\rho_{Ncross} = \tfrac{N_{cross}}{N_{e+}} = \tfrac{2J_+}{J_{e+}} = 2\left(\tfrac{R_0}{r}\right)^2\ \ \forall r> r_{cie}. \end{aligned} \tag{49}$$

Thus, for $n_i > n_e$ the solutions are significantly different from those for a nonscattering sphere and for a non-scattering sphere for $n_i \le n_e$. A special emphasis on the internal radiance that is uniform and isotropic only for $r \le r_{cie} = R_0\frac{n_e}{n_i}$. Moreover, both the fluence and the component of the internal partial flux along the radial direction are not longer uniform.

The internal average path length $\langle L\rangle$ can be obtained with the procedure described in Section 2.2 and by using the non-uniform fluence rate given by Eq. (45). However, the calculation of the integral of Eq. (20) is a bit cumbersome and the results can be more easily obtained from geometrical considerations together with Snell's and Fresnell's laws. Following the alternative procedure used for the slab geometry (see Appendix) we obtain for the

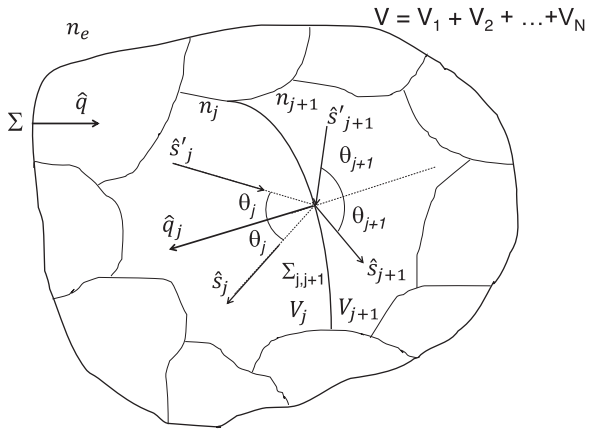


**Fig. 4.** Direction vectors for boundary condition for adjacent subvolumes $V_j$ and $V_{j+1}$: $\hat{s}_j$, $\hat{s}'_j$, $\hat{s}_{j+1}$, $\hat{s}'_{j+1}$, $\hat{q}_j$, are related by Snell's laws.

average path length $\langle L\rangle(\theta_e)$ for radiation with incidence angle over the sphere $\theta_e$:

$$\langle L\rangle(\theta_e) = 2R_0\cos\theta_i, \tag{50}$$

i.e. the same expression as for matched refractive index. Then, for $\langle L\rangle$ we obtain:

$$\begin{aligned}\langle L\rangle &= \frac{2\pi\int_0^{\pi/2}\langle L\rangle(\theta_e)I_0\cos\theta_e\sin\theta_e d\theta_e}{2\pi\int_0^{\pi/2}I_0\cos\theta_e\sin\theta_e d\theta_e} = 4R_0\int_0^{\pi/2}\cos\theta_i\cos\theta_e\sin\theta_e d\theta_e = \\ &= 4R_0\int_0^{\theta_{cie}}\cos\theta_i\left(\frac{n_i}{n_e}\right)^2\cos\theta_i\sin\theta_i d\theta_i = \\ &= \frac{4}{3}R_0\left(\frac{n_i}{n_e}\right)^2\left\{1-\left[1-\left(\frac{n_e}{n_i}\right)^2\right]^{3/2}\right\}.\end{aligned} \tag{51}$$

This solution is different from that for the scattering sphere and also from that the non-scattering sphere for $n_i \le n_e$ (Eq. (25)) because of the internal-external critical angle. Therefore, also for the non-scattering sphere with $n_i > n_e$ the invariance property does not apply. The same result has been also obtained by Majic et al. [30].

## 4. RTE for scattering volumes with non-uniform refractive index

The RTE solutions obtained in previous sections are for volumes with uniform refractive index. In this section, we show how to extend solutions to volumes with non-uniform discrete distributions of refractive index and where the scattering properties can vary in total generality.

### 4.1. Solutions for radiance and other radiometric quantities

With reference to Fig. 4, we consider an inhomogeneous volume $V$, without internal sources, enclosed by a smooth convex surface $\Sigma$ divided in a number $N$ of discrete sub-volumes $V_j$ of refractive index $n_j$ and with not restrictions on the scattering properties assumed inside each $V_j$. The surfaces enclosing each sub-volume is assumed to be smooth so that Snell's and Fresnel's law can be applied. The refractive index of the external medium is $n_e$ and the surface $\Sigma$ is illuminated by a CW Lambertian radiation.

To obtain a solution of the RTE, we have to solve the RTE in each volume $V_j$. Thus the radiance in each volume $V_j$, $I_j(\vec{r},\hat{s})$, is subjected to the CW RTE, i.e.:

$$\begin{aligned}&\nabla\cdot[I_j(\vec{r},\hat{s})\hat{s}] + \mu_s(\vec{r})I_j(\vec{r},\hat{s}) = \\ &= \mu_s(\vec{r})\int_{4\pi}p(\vec{r},\hat{s},\hat{s}')I_j(\vec{r},\hat{s}')d\hat{s}' \\ &\forall\vec{r}\in V_j \text{ and } \forall\hat{s},\end{aligned} \tag{52}$$

where $I_j$ is the radiance inside $V_j$. The boundary conditions at the external boundary $\Sigma$ are the same as Eqs. (5) and (6). Those on the surface $\Sigma_{j,j+1}$ separating the volumes $V_j$ and $V_{j+1}$ are

$$\begin{aligned}&I_j(\vec{r},\hat{s}_j) = R_{j,j+1}(\theta_j)I_j(\vec{r},\hat{s}'_j) + \\ &+T_{j+1,j}(\theta_{j+1})\left(\frac{n_j}{n_{j+1}}\right)^2 I_{j+1}(\vec{r},\hat{s}'_{j+1}) \\ &\forall\vec{r}\in\Sigma_{j,j+1} \text{ and } \hat{s}_j\cdot\hat{q}_j \ge 0,\end{aligned} \tag{53}$$

$$\begin{aligned}&I_{j+1}(\vec{r},\hat{s}_{j+1}) = R_{j+1,j}(\theta_{j+1})I_{j+1}(\vec{r},\hat{s}'_{j+1}) + \\ &+T_{j,j+1}(\theta_j)\left(\frac{n_{j+1}}{n_j}\right)^2 I_j(\vec{r},\hat{s}'_j) \\ &\forall\vec{r}\in\Sigma_{j,j+1} \text{ and } \hat{s}_{j+1}\cdot\hat{q}_j \le 0,\end{aligned} \tag{54}$$

where the unitary vectors $\hat{s}_j$, $\hat{s}'_j$, $\hat{s}_{j+1}$, $\hat{s}'_{j+1}$, $\hat{q}_j$ are related by Snell's laws. With these boundary conditions, whatever the internal scattering properties are, apart for non-scattering sub-volumes in which guided propagation can be established (see Section 3.2), the solution for the radiance inside $V_j$ is

$$I_j(\vec{r},\hat{s}) = \left(\frac{n_j}{n_e}\right)^2 I_0\ [\mathrm{Wm}^{-2}]\ \forall\hat{s} \text{ and } \forall\vec{r}\in V_j, \tag{55}$$

that depends on the refractive index $n_j$ internal to $V_j$ and $n_e$ external to $V$, but not on the refractive index of other sub-volumes. The solution for the outgoing radiance on the external boundary $\Sigma$ is:

$$I_e(\vec{r},\hat{s}) = I_0\ [\mathrm{Wm}^{-2}]\ \forall\vec{r}\in\Sigma \text{ and } \forall\hat{s}\,|\,-1\le\hat{s}\cdot\hat{q}\le 0. \tag{56}$$

It is interesting to observe that these solutions are very similar to those for the volume with uniform refractive index, i.e. Eqs. (9) and (10). In particular, for the outgoing radiation the two solutions are identical, with outgoing radiance, $I_e(\vec{r}_\Sigma,\hat{s})$, uniform, Lambertian, and with intensity identical to the incoming radiance. For the internal radiance Eq. (55) and Eq. (9) only differ for refractive index: $n_j$ for the sub-volume $V_j$ in Eq. (55), and $n_i$ for the total volume $V$ in Eq. (9). In both cases the radiance only depends on the ratio between the refractive index inside the considered sub-volume $V_j$ and the refractive index outside the volume $V$.

We also point out that, similarly to the solution for the volume with uniform refractive index (Eq. (9)), also the solution for the radiance inside any sub-volume $V_j$ with $\mu_{sj}\neq 0$ (Eq. (55)) is invariant both with respect to the geometry (size and shape of $V$ and of all the sub-volumes in which can be decomposed), with respect to the scattering properties (scattering coefficient, scattering function, homogeneity) of the whole volume $V$ and also with respect to the refractive index of all the other sub-volumes. In particular, Eq. (10) for the outgoing radiance also holds when all or part of the sub-volumes are non-scattering ($\mu_s(\vec{r})=0$) whatever the refractive index distribution is.

From Eqs. (55) and (56) we obtain:

$$\Phi_j(\vec{r}) = \int_{4\pi}I_j(\vec{r},\hat{s})d\hat{s} = 4\pi\left(\frac{n_j}{n_e}\right)^2 I_0,\ [\mathrm{Wm}^{-2}],\ \forall\vec{r}\in V_j, \tag{57}$$

$$\vec{J_j}(\vec{r}) = \int_{4\pi}I_j(\vec{r},\hat{s})\hat{s}d\hat{s} = 0,\ [\mathrm{Wm}^{-2}],\ \forall\vec{r}\in V_j, \tag{58}$$

$$J_{e+}(\vec{r}) = \pi I_0,\ [\mathrm{Wm}^{-2}]\ \forall\vec{r}\in\Sigma, \tag{59}$$

$$J_{j+}(\vec{r}) = -J_{j-}(\vec{r}) = \pi\left(\frac{n_j}{n_e}\right)^2 I_0,\ [\mathrm{Wm}^{-2}]\ \forall\vec{r}\in V_j, \tag{60}$$

$$\rho_{Ncross} = \frac{N_{cross\,j}}{N_{e+}} = \frac{2J_{j+}}{J_{e+}} = 2\left(\frac{n_j}{n_e}\right)^2\ \forall\vec{r}\in V_j. \tag{61}$$

As expected Eqs. (57)–(60) show that the invariance properties observed for the radiance also apply to the other radiometric quantities, i.e. solutions are invariant with respect to 1) the geometry, 2) the scattering properties of the whole volume $V$ and 3) the distribution of internal refractive index.

### 4.2. Solution for average internal path length

To obtain the average path length $\langle L_j \rangle$ followed inside $V_j$ we use the procedure of Section 2.2 for uniform refractive index: radiation $P_{jA1}$ absorbed inside $V_j$ in the limit of zero absorption is first evaluated by integrating the local absorption $\mu_a(\vec{r}_j)\Phi_j(\vec{r}_j)d\vec{r}_j$ over the volume $V_j$, and with the internal fluence of Eq. (57) we obtain

$$\lim_{\mu_a \to 0} P_{jA1} = \lim_{\mu_a \to 0} \int_{V_j} \mu_a(\vec{r}_j)\Phi(\vec{r}_j)d\vec{r}_j = \lim_{\mu_a \to 0} 4\pi\mu_a\left(\tfrac{n_j}{n_e}\right)^2 I_0 V_j. \quad (62)$$

It is then calculated the absorbed radiation $P_{jA2}$ in the limit of zero absorption using the probability density function $p_j(L_j)$ for path lengths followed inside $V_j$ by the total incoming radiation $\pi I_0 \Sigma$:

$$\lim_{\mu_a \to 0} P_{jA2} = \pi I_0 \Sigma \int_0^\infty \mu_a L_j p_j(L_j) dL_j = \pi I_0 \Sigma \mu_a \langle L_j \rangle (\mu_a = 0), \quad (63)$$

and equating Eqs. (62) and (63) the average internal path length results :

$$\langle L_j \rangle (\mu_a = 0) = 4\left(\tfrac{n_j}{n_e}\right)^2 \tfrac{V_j}{\Sigma}. \quad (64)$$

This expression is valid whatever the shape of the internal volume and whatever the internal optical properties are, apart for non-scattering sub-volumes ($\mu_s(\vec{r}_j) = 0$) when there are conditions for internal guided propagation. The average total path length $\langle L \rangle (\mu_a = 0)$ inside the total volume $V$ can be evaluated from the calculation of the total absorbed power by integrating the local absorption over the whole volume and by using the probability density function for total path length, or simply adding up the average internal path lengths of Eq. (64), i.e.

$$\langle L \rangle (\mu_a = 0) = \sum_{j=1}^{N} \langle L_j \rangle (\mu_a = 0) = 4 \sum_{j=1}^{N} \left(\tfrac{n_j}{n_e}\right)^2 \tfrac{V_j}{\Sigma}. \quad (65)$$

For the average path length only the invariance with respect to the scattering properties holds. Anyway, the dependence on the geometry for the average partial path length $\langle L_j \rangle (\mu_a = 0)$ is very simple and only involves the ratio between the volume $V_j$ of the considered sub-volume and the surface $\Sigma$ of the total volume $V$.

## 5. RTE for non-scattering volumes with non-uniform discrete refractive index distributions

For non-scattering and non-absorbing sub-volumes the RTE, Eq. (52), reduces to

$$\nabla \cdot [I_j(\vec{r}, \hat{s})\hat{s}] = 0 \ \ \forall \vec{r} \in V_j \text{ and } \forall \hat{s}, \quad (66)$$

where $I_j$ is the radiance inside $V_j$. The boundary conditions at the external boundary $\Sigma$ are the same as Eqs. (5) and (6) and those on the surface $\Sigma_{j,j+1}$ separating the volumes $V_j$ and $V_{j+1}$ are the same as Eqs. (53) and (54).

### 5.1. Solutions for radiance and other radiometric quantities

As for the non-scattering volume with constant refractive index, the solution also depends on the shape of the volume $V$ and of the sub-volumes $V_j$. Generally, multiple reflections are sufficient to re-establish the isotropic distribution of the radiance inside the sub-volumes and thus the solutions given in Section 4 are still valid. An exception is found for those sub-volumes where guided propagation can be established and thus where light can only propagate with incidence angles lower than the critical angle for $V_j$, $\theta_{cj}$. In consequence of this physical constrain, it will be $I_j(\vec{r}, \hat{s}) = 0$ for all $\forall \vec{r} \in V_j$ and for all $\hat{s}$ for which $\hat{s} \cdot \hat{q}_j > \theta_{cj}$. As examples of these kinds of exception, in the following we address two special examples: the layered non-scattering slab and sphere.

#### 5.1.1. Layered non-scattering slab

The solution of the RTE for a layered non-scattering slab expresses a limit physical condition where the absence of scattering implies that the trajectories are fully determined by reflections and refractions at the boundaries of the layers.

As for the homogeneous non-scattering slab the radiance for the layered slab is obtained from the boundary conditions on the external surface, Eqs. (5) and (6), and from the boundary conditions for adjacent layers, Eqs. (53) and (54). The solution for the internal radiance is:

$$\begin{aligned} &I_j(\vec{r}, \hat{s}) = \left(\tfrac{n_j}{n_e}\right)^2 I_0 \ \ \forall \vec{r} \in V_j \ \ \forall \hat{s} \,|\, |\hat{s} \cdot \hat{q}| \geq \cos\theta_{jMax} \\ &I_j(\vec{r}, \hat{s}) = 0 \ \ \forall \vec{r} \in V_j \, \forall \hat{s} \,|\, |\hat{s} \cdot \hat{q}| < \cos\theta_{jMax}, \end{aligned} \quad (67)$$

where $I_0$ is the radiance on the external surface $\Sigma$, $\hat{q}$ is the unit vector perpendicular to the slab external sides inwardly directed, $\theta_{jMax}$ is the maximum angle with which radiation from the external boundary can penetrate inside the $j$th layer:

$$\sin\theta_{jMax} = \text{MAX}\left[\sin(\theta_{jMaxTop}), \sin(\theta_{jMaxBot})\right] \quad (68)$$

with $\theta_{jMaxTop}$ and $\theta_{jMaxBot}$ maximum angle respectively for radiation from the top and from the bottom of the $j$th layer of the slab, given by:

$$\begin{aligned} &\sin\theta_{jMaxTop} = \text{MIN}\left[1, \tfrac{n_{j-1}}{n_j}\sin(\theta_{j-1MaxTop})\right] \\ &\sin\theta_{jMaxBot} = \text{MIN}\left[1, \tfrac{n_{j+1}}{n_j}\sin(\theta_{j+1MaxBot})\right], \end{aligned} \quad (69)$$

and for the first layer ($j = 1$) and the last layer ($j = N$):

$$\begin{aligned} &\sin\theta_{1MaxTop} = \text{MIN}\left[1, \tfrac{n_e}{n_1}\right] \\ &\sin\theta_{NMaxBot} = \text{MIN}\left[1, \tfrac{n_e}{n_N}\right]. \end{aligned} \quad (70)$$

Solutions for fluence, flux, partial flux and "crossing density" are:

$$\Phi_j(\vec{r}) = 4\pi\left(\tfrac{n_j}{n_e}\right)^2 I_0\left[1 - \cos(\theta_{jMax})\right], \ [\text{Wm}^{-2}] \, \forall \vec{r} \in V_j, \quad (71)$$

$$\vec{J_j}(\vec{r}) = 0 \ \forall \vec{r} \in V_j, \quad (72)$$

$$J_{e+}(\vec{r}) = -J_{e-}(\vec{r}) = \pi I_0, \ [\text{Wm}^{-2}] \, \forall \vec{r} \in \Sigma, \quad (73)$$

$$J_{j+}(\vec{r}) = -J_{j-}(\vec{r}) = \pi\left(\tfrac{n_j}{n_e}\right)^2 I_0 \sin^2(\theta_{jMax}), \ [\text{Wm}^{-2}] \, \forall \vec{r} \in V_j, \quad (74)$$

$$\rho_{Ncross} = \tfrac{N_{cross}}{N_{e+}} = \tfrac{2J_+}{J_{e+}} = 2\left(\tfrac{n_j}{n_e}\right)^2 \sin^2(\theta_{jMax}) \text{ in layer } j. \quad (75)$$

The obtained solutions for the non-scattering layered slab differ from the case of a scattering layered slab by a multiplicative term that accounts for the maximum incidence angle on layer $j$.

To obtain the average path length $\langle L_j \rangle$ followed inside the layer $j$ we follow the same procedure of Section 4. With $\Phi_j$ given by Eq. (71), the radiation $P_{jA1}$ absorbed inside the volume $V_j$ for the layer $j$ in the limit of zero absorption, obtained by integrating the local absorption $\mu_a(\vec{r})\Phi_j(\vec{r})d\vec{r}$ over the volume $V_j$, is

$$\begin{aligned} &\lim_{\mu_a \to 0} P_{jA1} = \lim_{\mu_a \to 0} \int_{V_j} 4\pi\mu_a\left(\tfrac{n_j}{n_e}\right)^2 I_0\left[1 - \cos(\theta_{jMax})\right] d\vec{r} = \\ &= \lim_{\mu_a \to 0} 4\pi\mu_a\left(\tfrac{n_j}{n_e}\right)^2 I_0 V_j\left[1 - \cos(\theta_{jMax})\right]. \end{aligned} \quad (76)$$

The formal expression for the absorbed radiation $P_{jA2}$ obtained from the probability density function for path lengths followed inside $V_j$ by the total incoming radiation is identical to that of Eq. (63). Equalizing Eq. (76) and Eq. (63) the average internal path length $\langle L_j \rangle$ results

$$\langle L_j \rangle (\mu_a = 0) = 2s_j\left(\tfrac{n_j}{n_e}\right)^2\left[1 - \cos(\theta_{jMax})\right]. \quad (77)$$

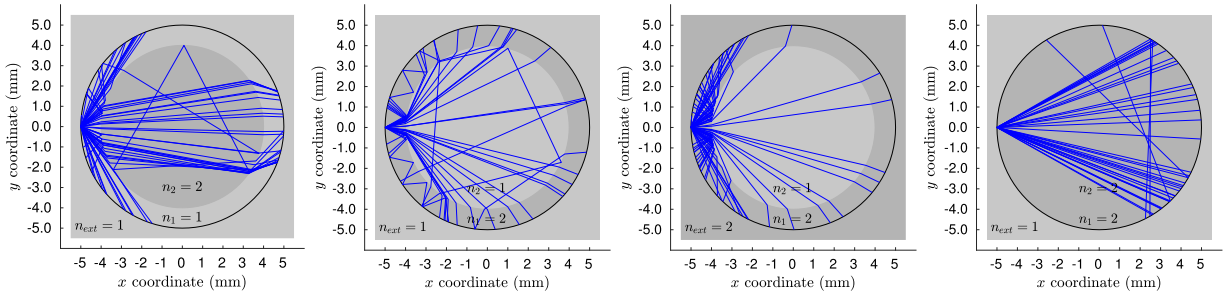


**Fig. 5.** Examples of photons trajectories through a two layer non-scattering sphere. The refractive indices of the external medium and of the internal layers are shown in the inset of the figures. The figures shows some trajectories extracted for a layered sphere of 5 mm radius in which the layers are highlighted in the figures. The boundary of the layers are at a distance of 4 and 5 mm from the centre of the sphere.

where $s_j$ is the thickness of the $j$th layer. Also the mean path length spent in the layer $j$ differs from the case of a scattering layered slab by a multiplicative term that accounts for the maximum incidence angle on layer $j$.

Solutions for non-scattering slab with layered refractive index can be useful for instance for validating algorithms to manage reflections and refractions in MC codes for layered slab.

*5.1.2. Layered non-scattering sphere*

Let's assume to have a layered non-scattering sphere, composed of concentric spherical layers, with a discrete number of layers of radius $R_j$ and refractive index $n_j$ (with the convention that $R_j > R_{j+1}$).

Figure 5 shows examples of trajectories in a two layer sphere for two combinations of the refractive index. The refractive indices are shown in the inset of the figures.

As for layered non-scattering slab, the internal radiance $I_j(\vec{r},\hat{s})$ in the layer $j$ is obtained from the boundary conditions on the external surface, Eqs. (5) and (6), and from the boundary conditions for adjacent layers, Eqs. (53) and (54). It results that the internal radiance is:

$$\begin{aligned} I_j(\vec{r},\hat{s}) &= \left(\tfrac{n_j}{n_e}\right)^2 I_0 \;\; \forall \vec{r} \in V_j \;\forall\; \hat{s} \,|\, \arccos[|\hat{s}\cdot\hat{q}(\vec{r})|] \le \theta_{jMax}(r) \\ I_j(\vec{r},\hat{s}) &= 0 \;\; \forall \vec{r} \in V_j \;\; \forall \hat{s} \,|\, \arccos[|\hat{s}\cdot\hat{q}(\vec{r}_j)|] > \theta_{jMax}(r), \end{aligned} \tag{78}$$

where $\hat{q}(\vec{r})$ is the inwardly directed normal to the sphere with radius $r$ and

$$\theta_{jMax}(r) = \arcsin\left[\mathrm{MIN}\left(1, \tfrac{r_{jc}}{r}\right)\right], \tag{79}$$

with

$$r_{jc} = R_j \sin\theta_{jIn}, \tag{80}$$

and

$$\begin{aligned} \sin\theta_{1In} &= \mathrm{MIN}\left[1, \tfrac{n_e}{n_1}\right], \\ \sin\theta_{jIn} &= \mathrm{MIN}\left[1, \tfrac{n_{j-1}}{n_j}\sin\theta_{j-1Out}\right], \\ \sin\theta_{jOut} &= \mathrm{MIN}\left[\left(1, \tfrac{r_{jc}}{R_j}\right)\right]. \end{aligned} \tag{81}$$

The angles $\theta_{jIn}$ and $\theta_{jOut}$ represent respectively the maximum refracted angle on the external surface (radius $R_j$) and the maximum incidence angle on the internal surface (radius $R_{j+1}$) of the $j$th layer. The corresponding expressions for fluence and fluxes are:

$$\Phi_j(\vec{r}) = 4\pi\left(\tfrac{n_j}{n_e}\right)^2 I_0\left[1-\cos\theta_{jMax}(r)\right], \;\; \forall \vec{r} \in V_j \tag{82}$$

$$\vec{J_j}(\vec{r}) = 0, \;\; \forall \vec{r} \in V_j \tag{83}$$

$$J_{e+}(R_1) = \pi I_0, \;\; [\mathrm{Wm}^{-2}] \;\; \forall \vec{r} \in \Sigma, \tag{84}$$

$$J_{j+}(\vec{r}) = -J_{j-}(\vec{r}) = \pi\left(\tfrac{n_j}{n_e}\right)^2 I_0 \sin^2\theta_{jMax}(r), \;\; \forall \vec{r} \in V_j, \tag{85}$$

$$\rho_{Ncross} = \frac{N_{cross}}{N_{e+}} = \frac{2J_+(r)}{J_{e+}} = 2\left(\frac{n_j}{n_e}\right)^2 \sin^2\theta_{jMax}(r) \;\; \forall r \,\text{in layer}\, j. \tag{86}$$

The obtained solutions for the non-scattering layered sphere differ from the case of a scattering layered sphere by a multiplicative term that accounts for the maximum incidence angle on layer $j$.

Also solutions for non-scattering sphere with layered refractive index can be useful for instance for validating algorithms to manage reflections and refractions in MC codes.

In case that only some layers are non-scattering, solutions for scattering layers are identical to those discussed for the layered scattering medium (for these layers the RTE is that of Eq. (66)). Similarly, for non-scattering layers solutions presented in this section for the sphere and in the previous one for the slab remain valid. Obviously in calculating $\theta_{jMax}$, the maximum angle with which radiation from the external boundary $\Sigma$ can penetrate inside the $j$th layer (Eq. (68) for the slab, Eq. (79) for the sphere), we should take into account that the radiance inside any scattering layer is uniform and isotropic accordingly to the obtained solutions.

## 6. Discussion

Although the invariance property is known since many years, it is difficult to find in literature a complete presentation of this subject. To the best of our knowledge this is the first work where the path length invariance property of disordered scattering media has been derived in all generality from RTE under the assumption of uniform Lambertian illumination. More importantly, we have shown that invariance properties can be derived for the radiance, the fluence and the flux with a larger extent range of situations.

On this ground, we have provided in all generality the solutions of the RTE for non-absorbing scattering volumes illuminated by uniform Lambertian radiation. In this work we have also presented solutions for non-scattering inhomogeneous volumes that have not been considered in the previous literature. These solutions offer a powerful tool to deeply understand the complexity of light propagation and to realize at the same time the ease and intuitiveness of the approach here proposed. Indeed, in many applied fields such as tissue optics, except few cases [3–13], it is still claimed a lack of easy tractable solutions of the RTE.

In the previous sections, we have presented the exact solution of the RTE for the radiance and other radiometric quantities for a non-absorbing volume illuminated with uniform and Lambertian CW radiation on the external surface (Sections 2.1, 2.2, 4.1 and 4.2). The solutions have been at first obtained for a volume with a uniform refractive index (Sections 2.1 and 2.2) and then generalized

to a volume with a variable (discrete variations of) refractive index (Sections 4.1 and 4.2). All solutions are obtained in a simple way and with elementary mathematics. The only constrains for their validity are: 1) the external surface of the illuminated volume, that must be smooth and convex, 2) the external medium, that must be non-scattering and with uniform refractive index, and 3) the internal scattering coefficient must be non-null for sub-volumes in which there are conditions for guided propagation. In fact, even though the formulas (Sections 2, 4) were derived for scattering media, they are also valid under this more general condition. In other words, they are valid also for regions of null scattering as long as guided propagation cannot occur. The condition of guided propagation only occurs when there are particular symmetries, as for slab or sphere with a layered refractive index or with refractive index mismatch with the external volume. For these geometries, often of interest, solutions for non-scattering layers have also been obtained in two different ways, solving the RTE (Sections 3.2.1 and 3.2.2) or resorting to Snell's and Fresnell's laws (see Appendix). These invariance properties also apply to the outgoing radiation $I_e\left(\vec{r},\hat{s}\right)$, that is always uniform and Lambertian (also in presence of sub-volumes with $\mu_s = 0$ in which there are conditions for guided propagation).

Solutions for all radiometric quantities inside any sub-volume $V_j$ internal to the illuminated volume $V$ show interesting invariance properties. Solutions only depend on the refractive index mismatch between the sub-volume index $n_j$ and the external medium index $n_e$. Solutions are therefore invariant with respect to: 1) the scattering properties, i.e. both the scattering coefficient and the scattering function can vary in all generality (the only constrain is $\mu_s \neq 0$ for sub-volumes with conditions for guided propagation); 2) for an internal sub-volume, the refractive index of other sub-volumes; 3) the geometry, i.e., size and shape of the illuminated volume and of internal sub-volumes (the only constrain is on the external surface that must be smooth and convex).

Although the RTE has been only solved for CW sources, some general information has been obtained also on the length of paths followed by photons into the volume. This has been possible thanks to the strict relationship between the internal fluence and the mean path length followed by photons used in Sections 2.2 and 4.2. From the solutions for the fluence we have obtained the mean path length followed by photons both in a volume with uniform refractive index, $\langle L\rangle$, and in a sub-volume $V_j$ with refractive index $n_j$, $\langle L_j\rangle$. The invariance properties of the radiometric quantities with respect to the scattering properties and the refractive index are also valid for the mean path length. As for the dependence on the geometry, the mean pathlenght only depends on the ratio between the volume $V_j$ and the area of the illuminated external surface $\Sigma$.

We point out that the invariance of $\langle L\rangle$ with respect to the scattering properties for the volume with uniform refractive index is the well known invariance property widely investigated also in recent years [14–20,22,23]. We also note that solutions for $\langle L\rangle$ in homogeneous non-scattering slab, sphere, infinite cylinder, cube and also for other 3D and 2D geometries have been recently described in Ref. [30] using a quite general approach for the non-scattering case. For the slab, the procedure used in Ref. [30] is very similar to that used in the Appendix. However, it is important to note the very different perspectives of this work compared to Ref. [30]. Whilst Ref. [30] considers only the non-scattering case and the information on mean path-length, the present work addresses scattering and non scattering media, homogeneous and inhomogeneous media, obtaining solutions not only for the mean path length but also for all the radiometric quantities. Moreover, our procedure is within the frame of the RTE, while Ref. [30] is based on geometrical optics and thermodynamics considerations. Thus, the two works overlap only in few results obtained for the mean path length in non-scattering media, while for all the other aspects provide different views, approaches and investigations. It is also worth to note that Ref. [30] discusses real physical systems where exact zero values cannot be encountered both for the absorption and scattering coefficients. On the contrary we are concerned with the mathematical solutions of RTE in general situations, including also the ideal ones of non-absorbing and non-scattering media. The solutions described in this work, even though obtained in ideal conditions, offer an important reference for testing numerical and/or analytical algorithms for light propagation under the validity of RTE. A practical example can be for instance the validation of MC or finite element method (FEM) codes for which exact reference are very few and only for very simple and specific geometries [31,32].

In our opinion there is another important application for the solutions here described: The invariance with respect to the scattering properties, the geometry, and the refractive index implies that the same identical results for all the radiometric quantities are obtained in a large number of situations, with extremely different regimes of propagation. Therefore, there is a large variety of propagation regimes, each one of great complexity, that gives rise to the same identical internal lighting conditions, all exactly described by the same, simple, solution. Indeed, this result is counterintuitive, as well as also important and very useful. For instance, it provides a unique introduction to the world of light propagation through scattering media that emphasizes and highlights the two-fold aspect of the presented approach where the complexity of the propagation regimes and the simplicity of the solutions coexist.

To give an example of the variety of physical situations with identical RTE solutions we refer to Figs. 6-7. These figures pertain to a sphere of radius 5 mm, with uniform optical properties (scattering coefficient and scattering function) and with a layered refractive index distribution (four layers, see Tables 1). The results pertain to a unitary incident flux $J_{e+}$ of 1 Wmm$^{-2}$. The figures refer to two profiles of refractive index, DwUp and UpDw, shown in Tables 1. In Tables 1 the values of RTE solutions in the layers for the profiles DwUp and UpDw and for $\mu_s \neq 0$ are summarized. Light propagation for the two profiles is significantly different: for DwUp we have 59.6% of the impinging radiation reflected on the external surface and $\langle L\rangle = 4.296$ mm; for UpDw only 6.65% of radiation is reflected and $\langle L\rangle = 9.985$ mm. However, predictions of the RTE solutions (radiance and fluence) for layers $j = 2$ and $j = 4$ are identical for the two profiles.

Figures 6 and 7 pertain to the total path length probability distribution function, PDF($L$), followed by photons respectively for the profiles DwUp and for the UpDw (see Tables 1) obtained with MC simulations [2,33]. To show the strong influence of scattering on propagation, examples of path length probability distribution function (PDF) are displayed for different values of $\mu_s$ ranging from 0 to 2 mm$^{-1}$ and scattering function obtained with the Henyey and Greenstein model with asymmetry factor $g = 0$. It is worth to note that, despite the strong differences in the probability distribution function, the mean value of $L$ remains the same in scattering media with the same profile of refractive index. The curves with many spikes for $\mu_s = 0$ are only determined by multiple reflections/refractions. On the contrary, the smooth curves for $\mu_s \geq 1$ mm$^{-1}$, are mainly determined by multiple scattering and thus pertain to a diffusive regime of propagation. Curves for $\mu_s = 0.01$ and 0.1 mm$^{-1}$ pertain to an intermediate regime in which the contribution of trajectories only determined by reflections/refractions and that of trajectories with few orders of scattering has similar importance.

The PDF curves, for each profile of refractive index, are very different versus the value of the scattering coefficient $\mu_s$. However, as predicted by the RTE solutions, the corresponding overall illuminations within the sphere are identical, with identical radiance dis-

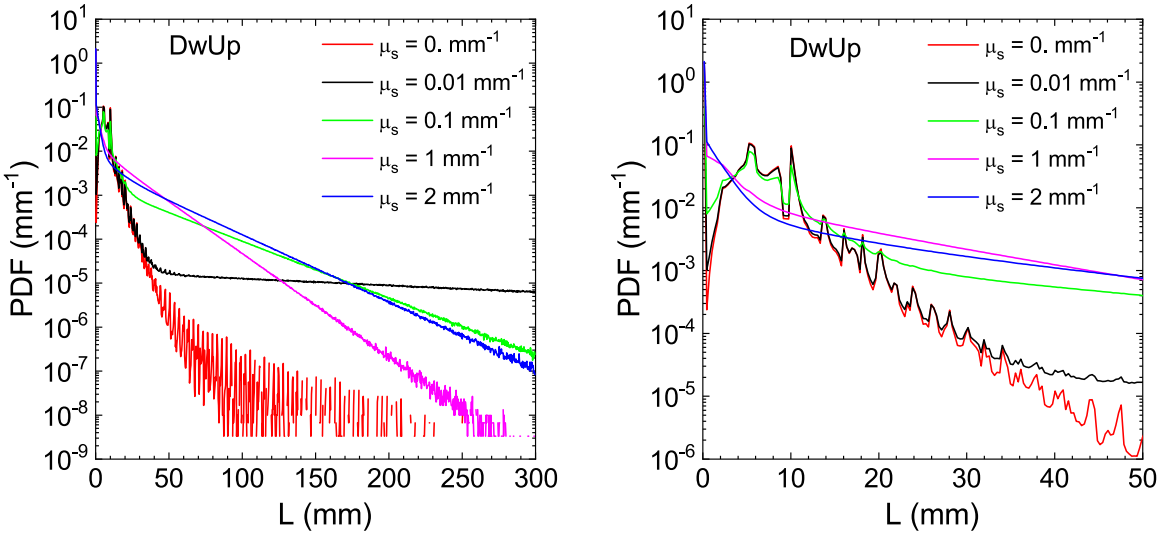


**Fig. 6.** Path length probability distribution function, PDF($L$), versus the length $L$ obtained with MC simulations for the profile DwUp and some values of $\mu_s$. The right panel is the zoomed in version of the left panel.

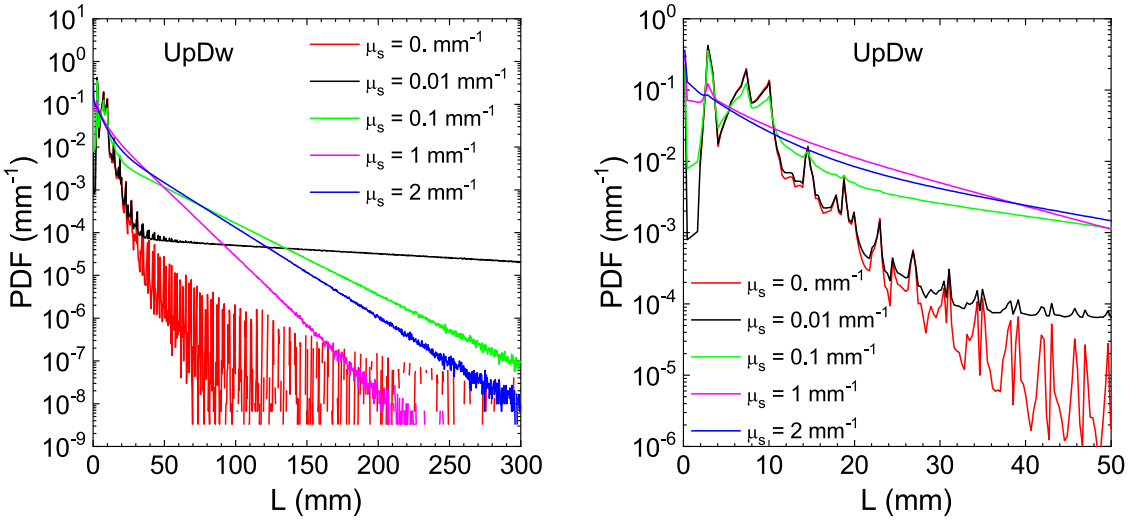


**Fig. 7.** Path length probability distribution function, PDF($L$), versus the length $L$ obtained with MC simulations for the profile UpDw and some values of $\mu_s$. The right panel is the zoomed in version of the left panel.

**Table 1**
The table shows the RTE solutions in a four-layered sphere for two profiles of refractive index DwUp and UpDw and with $\mu_s \neq 0$ and constant. The index $e$ indicates the external medium. Solutions of the RTE for $\langle L_j \rangle$ (total path length in layer $j$), $I_j$ (radiance in layer $j$), $\Phi_j$ (fluence in layer $j$) and $\langle L \rangle$ (total mean path length) are reported. The average reflection coefficient for Lambertian radiation on the external surface $\langle R_L \rangle$ is also shown. The symbols $R_j$ and $n_j$ indicate the external radius and refractive index of the layer $j$, respectively.

| | Layer $j$ | $e$ | 1 | 2 | 3 | 4 | | |
|---|---|---|---|---|---|---|---|---|
| | $R_j$ (mm) | | 5 | 4 | 3 | 2 | $\langle R_L \rangle$ | $\langle L \rangle$ (mm) |
| DwUp | $n_j$ | 1.5 | 1 | 1.5 | 1 | 1.5 | 0.5963 | 4.2963 |
| | $\langle L_j \rangle$ (mm) | | 1.4459 | 1.9733 | 0.4504 | 0.4267 | | |
| | $I_j$ (Wmm$^{-2}$) | | 0.1415 | 0.3183 | 0.1415 | 0.3183 | | |
| | $\Phi_j$(Wmm$^{-2}$) | | 1.7778 | 4 | 1.7778 | 4 | | |
| UpDw | $n_j$ | 1.5 | 2 | 1.5 | 2 | 1.5 | 0.0665 | 9.9852 |
| | $\langle L_j \rangle$ (mm) | | 5.7837 | 1.9733 | 1.8015 | 0.4267 | | |
| | $I_j$ (Wmm$^{-2}$) | | 0.5659 | 0.3183 | 0.5659 | 0.3183 | | |
| | $\Phi_j$(Wmm$^{-2}$) | | 7.1111 | 4 | 7.1111 | 4 | | |

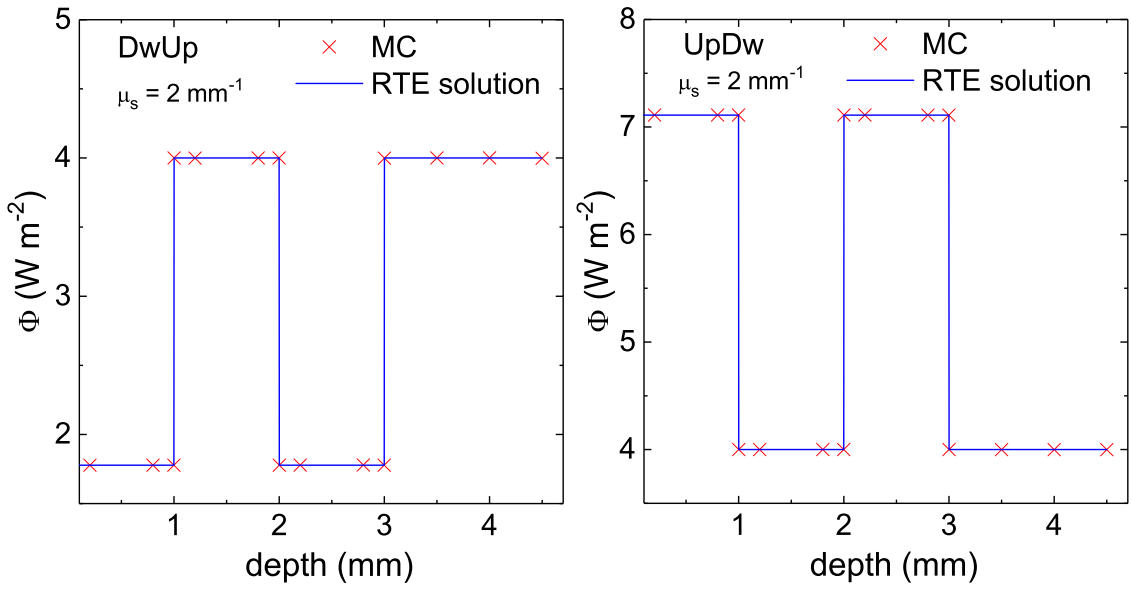


**Fig. 8.** Fluence rate for the two profiles DwUp and UpDw for $\mu_s = 2$ mm$^{-1}$. The figures shows the results of MC simulations (marks) and the RTE solution (curves). The fluence is plotted against the depth from the external surface of the sphere.

tribution and identical mean path length in each layer, whatever scattering strength is considered. The only exception is for layers $j = 1$ and $j = 3$ for the UpDw profile with $\mu_s = 0$, in which there are conditions for internal guided propagation.

Since the two profiles have identical refractive index for the external medium $n_e$ and for layers $j = 2$ and $j = 4$, identical solutions are also predicted for the two profiles in these layers. As also shown by MC simulations (results not reported), identical results for all CW radiometric quantities and for internal mean path length have been obtained with different distribution both for the scattering properties and for the refractive index in spite of very different propagation regimes with very different PDF. In Fig. 8, as an example, it is shown the fluence for the profiles DwUp and UpDw for $\mu_s = 2$ mm$^{-1}$. In figure the results of the MC simulation and of the RTE solution are shown. The figure offers an overview of the expected profile from the RTE solution and MC simulations accordingly to the two profiles of refractive index DwUp and UpDw of Tables 1.

## 7. Conclusions

We have examined with a quite large view the invariance properties of RTE solutions in non-absorbing media subjected to Lambertian illumination. It is worth to further remind that also the solution for the outgoing radiation $I_e(\vec{r}, \hat{s})$ is invariant with respect to the geometry, the scattering properties and the refractive index distribution. The outgoing radiance is uniform, Lambertian and with intensity identical to the incoming radiance. It can be finally noted that for the geometries of slab and sphere, given the symmetry of these geometries, the RTE solutions for the mean path length are also valid for a point-like Lambertian illumination provided that the detected light is collected from the whole external surface.

It is interesting to observe that the RTE solutions obtained for non-absorbing volumes with non-uniform distributions of refractive index are very similar to those for volumes with uniform distributions of refractive index (Eqs. (9) and (10)). In particular, for the outgoing radiation solutions are identical, with an outgoing radiance $I_e(\vec{r}_\Sigma, \hat{s})$, uniform, Lambertian, and with intensity identical to the incoming radiance. This fact implies that a re-emission of Lambertian radiation is always possible from any medium illuminated by a uniform Lambertian illumination. The solutions presented in our work implicitly provide a sufficient condition of existence of a Lambertian surface. Thus, in the light of the presented results, we can argue that a Lambertian surface does exist whether it is possible to illuminate a non-absorbing volume with a uniform Lambertian light. Under the condition of uniform Lambertian illumination, a non-absorbing volume at its external surface becomes a Lambertian surface.

The solutions of the RTE and their invariance properties under the conditions of Lambertian illumination emphasize that the physical origin of this regime of propagation is the uniform and isotropic distribution of the radiance inside the medium and the uniform distribution of the fluence rate. Moreover, also the crossing density of photons inside any internal surface of the medium results to be a uniform quantity that only depends on the refractive index mismatch between internal and external medium. Whenever the light propagation can assure these two conditions the invariance property holds. In case the medium is characterized by an inhomogeneous discrete distribution of refractive index the above physical insight remains valid inside each sub-domain where the refractive index of the medium is constant.

The invariance properties of the obtained RTE solutions versus the scattering properties, for the reflectance and the other radiometric quantities, for a non-absorbing volume illuminated with Lambertian uniform radiation, emphasize the intrinsic difficulties to re-construct the scattering properties of volumes from measurements of radiometric quantities especially when determined in a multiple scattering regime of propagation.

In particular, we can state that, for the case of CW Lambertian illumination of a scattering medium (i.e. the incident radiance is constant at each point of its boundary), we cannot recover its scattering properties from measurements of radiometric quantities taken on the surface of the medium or inside it. However, from CW measurements of radiometric quantities inside the volume, such as fluence, radiance and mean path length, we can retrieve the distribution of the refractive index.

Only with the introduction of absorption inside the volume or by breaking the condition of uniform illumination, it possible to have information on the scattering properties. The presence of absorption makes all the radiometric quantities dependent from scattering and establishes relations among them. Thus, in an absorbing

medium is possible to re-construct both absorption and scattering properties from radiometric CW measurements also when the volume is uniformly illuminated. A general intrinsic difficulty to retrieve the optical properties remains the lack of exact solutions of the RTE in absorbing volumes and to the existing correlation between scattering and absorption effects, as for instance in the approximate solutions of the diffusion equation [2].

The uniform illumination can be "broken" both in time and in space. In the first case we note that information can be gained from time-resolved measurements. However, we point out that the existing time-resolved solutions of RTE are complex also for regularly bounded geometries. For scattering and absorbing media, the shape of the Temporal Point Spread Function at late times is basically determined by the absorption coefficient, whilst the information on the scattering coefficient is encoded inside the early photons. Thus, their detection may require a high temporal resolution making this task particularly difficult.

The uniform illumination can be also "broken" by using radiation uniform in time, but not in space, as for instance by illuminating the boundary of the medium with a CW pencil beam. In this case the dependence on the scattering properties is encoded inside the spatial distribution of the radiance, and the re-construction of the scattering properties can be obtained from spatially resolved CW measurements (reflectance measurements on the boundary or fluence measurements inside the volume). However, also in this case difficulties can be emphasized due to the lack of exact RTE solutions for this kind of illumination and to the strong correlation between scattering and absorption effects, particularly evident in the solutions of the diffusion equation [2].

With the above overview we have represented the scenario of the retrieval of the optical properties in scattering media. The condition of uniform Lambertian illumination offers a clear and powerful interpretation of the intrinsic difficulties to perform this task. It is impressive how all the vision can be derived from an initial regime of propagation, the one addressed in this paper, i.e. a uniform CW Lambertian illumination, where the uniform characteristic of the illumination is maximum. This fact emphasizes the importance of the RTE solutions presented in this paper. It is also important to stress that the presented solutions are valid also for Levy flight materials [34]. In fact these materials, that present interesting properties of anomalous transport, are made with a proper choice of inhomogeneous components and then are within the cases presented in this work.

Finally, we observe that the presented exact solutions can find in future a use as "reference standard" for analytical models or numerical simulations aimed to make predictions on radiative transport calculations. Indeed, the expanded domain of validity of the invariance properties of the solutions of the radiative transfer in condition of Lambertian illumination offers a unique reference standard, known with arbitrary accuracy, for the validation of computational codes used in photon migration in diffusive media, such as Monte Carlo and finite element methods or any other numerical and analytical method.

## Declaration of Competing Interest

The authors declare that they have no known competing financial interests or personal relationships that could have appeared to influence the work reported in this paper.

## CRediT authorship contribution statement

**Fabrizio Martelli:** Conceptualization, Methodology, Software, Investigation, Writing – original draft, Writing – review & editing, Visualization, Supervision. **Federico Tommasi:** Conceptualization, Methodology, Software, Investigation, Writing – original draft, Writing – review & editing, Visualization. **Lorenzo Fini:** Conceptualization, Methodology, Investigation, Writing – review & editing. **Lorenzo Cortese:** Conceptualization, Methodology, Investigation, Writing – review & editing. **Angelo Sassaroli:** Conceptualization, Methodology, Investigation, Writing – review & editing. **Stefano Cavalieri:** Conceptualization, Methodology, Investigation, Writing – original draft, Writing – review & editing.

## Acknowledgements

The authors wish to thank prof. Giovanni Zaccanti for useful suggestions and Dr. André Liemert for useful discussions. The authors wish to acknowledge support from Ente Cassa di Risparmio di Firenze grant 2020. Lorenzo Cortese wishes to acknowledge European Union's Horizon 2020 research and innovation programme (grant agreement No. 688303, LUCA-project) as an initiative of the Photonics Public Private Partnership (www.photonics21.org) and Fundació CELLEX Barcelona. Angelo Sassaroli wishes to acknowledge support from the National Institutes of Health, Grant No. R01 NS095334.

## Appendix

*Solutions for the slab with $\mu_s(\vec{r}) = 0$ and $n_i > n_e$ based on Snell's and Fresnel's laws*

It may be also interesting to show how solutions for the non-scattering slab can be obtained following a different approach only based on Snell's and Fresnel's laws. With reference to Fig. 2, the radiance on a surface element (boundary of the slab $\Sigma$) can be obtained summing the transmitted component and the multiple reflections components:

$$I\left(\vec{r}_\Sigma, \hat{s}\right) = I_0 T_{ei}(\theta_e)\left(\tfrac{n_i}{n_e}\right)^2 \sum_{n=0}^{\infty} R_{ie}^n(\theta_i), \tag{87}$$

where $T_{ei}(\theta_e)$ is the external to internal transmission coefficient, $R_{ie}(\theta_i)$ is the internal to external reflection coefficient, $I_0$ the radiance on the external surface and $\left(\frac{n_i}{n_e}\right)^2$ accounts for the different geometrical extent of the beam element inside and outside the slab. Since the previous series is a power series,

$$\sum_{n=0}^{\infty} R_{ie}^n(\theta_i) = \frac{1}{1 - R_{ie}(\theta_i)} = \frac{1}{T_{ie}(\theta_i)}, \tag{88}$$

and also $T_{ie}(\theta_i) = T_{ei}(\theta_e)$, we obtain for the internal radiance:

$$\begin{aligned} &I\left(\vec{r}, \hat{s}\right) = \left(\tfrac{n_i}{n_e}\right)^2 I_0, \quad \forall \vec{r} \in V, \quad \forall \hat{s} \,|\, |\hat{s} \cdot \hat{q}| \geq \cos\theta_{cie} \quad \left(\sin\theta_{cie} = \tfrac{n_e}{n_i}\right) \\ &I\left(\vec{r}, \hat{s}\right) = 0, \quad \forall \hat{s}| \ |\hat{s} \cdot \hat{q}| < \cos\theta_{cie}. \end{aligned} \tag{89}$$

This solution is identical to the solution obtained from the boundary conditions (Eqs. (35) and (36)). It is interesting to observe that for directions with $\theta_i \leq \theta_c$ it is $I\left(\vec{r}, \hat{s}\right) = \left(\frac{n_i}{n_e}\right)^2 I_0$ independent of the incidence angle $\theta_e$ despite that the transmission coefficient $T_{ei}(\theta_e)$ depends on $\theta_e$. This is because the reflected radiation lost on the external surface is exactly compensated by multiple reflections coming from other surface elements (to visualize the effect may help Fig. 2). Because of this perfect compensation the internal radiance is only determined by the variation of the beam element extension passing from outside to inside.

Also the internal average path length $\langle L \rangle$ can be obtained from geometrical considerations together with Snell's laws. We first evaluate the average path length $\langle L \rangle(\theta_e)$ for radiation with incidence angle $\theta_e$ as the weighted sum of the lengths followed by radiation leaving the slab after multiple reflections:

$$\langle L \rangle(\theta_e) = 0 \cdot R_{ei}(\theta_e) + \tfrac{s_0}{\cos\theta_i}\left[T_{ei}(\theta_e) T_{ie}(\theta_i) \sum_{n=0}^{\infty} (n+1) R_{ie}^n(\theta_i)\right], \tag{90}$$

where the weight factor $T_{ei}(\theta_e)T_{ie}(\theta_i)R_{ie}^n(\theta_i)$ is the fraction of radiation with path length $\frac{(n+1)s_0}{\cos\theta_i}$ leaving the slab after $n$ internal reflections, i.e., probability of radiation incident at angle $\theta_e$ to travel a path length $\frac{(n+1)s_0}{\cos\theta_i}$ inside the slab. Let's introduce the path length $Ln$, and its discrete probability, $P(Ln)$, defined as follow:

$$\begin{aligned} &Ln = \tfrac{(n+1)s_0}{\cos\theta_i}, \\ &P(Ln) = T_{ei}^2 R_{ei}^n, \\ &P(Ln=0) = R_{ei}. \end{aligned} \tag{91}$$

Since $R_{ei}(\theta_e) = R_{ie}(\theta_i)$ and $T_{ei}(\theta_e) = 1 - R_{ei}(\theta_e) = T_{ie}(\theta_i)$, we have that $P(Ln=0) + \sum_{n=0}^{\infty} P(Ln) = 1$. In fact:

$$R_{ei} + \left[T_{ei}^2 \sum_{n=0}^{\infty} R_{ei}^n\right] = R_{ei} + \left[(1-R_{ei})^2 \tfrac{1}{1-R_{ei}}\right] = 1. \tag{92}$$

The weights' distribution is thus normalized. Furthermore, since

$$\sum_{n=0}^{\infty} (n+1) R_{ie}^n(\theta_i) = \tfrac{1}{1-R_{ie}(\theta_i)} + \tfrac{R_{ie}(\theta_i)}{1-R_{ie}(\theta_i)^2}, \tag{93}$$

we obtain

$$\langle L\rangle(\theta_e) = \tfrac{s_0}{\cos\theta_i}, \tag{94}$$

similar to the expression for matched refractive index. The total average path length $\langle L\rangle$ is obtained as

$$\langle L\rangle = \tfrac{2\pi \int_0^{\pi/2} \langle L\rangle(\theta_e) I_0 \cos\theta_e \sin\theta_e d\theta_e}{2\pi \int_0^{\pi/2} I_0 \cos\theta_e \sin\theta_e d\theta_e}. \tag{95}$$

Then, by using Eq. (94) we can express $\langle L\rangle$ as:

$$\begin{aligned} \langle L\rangle &= s_0\, 2 \int_0^{\pi/2} \tfrac{1}{\cos\theta_i} \cos\theta_e \sin\theta_e d\theta_e = \\ &= s_0\, 2 \int_0^{\theta_{cie}} \tfrac{1}{\cos\theta_i} \left(\tfrac{n_i}{n_e}\right)^2 \cos\theta_i \sin\theta_i d\theta_i = \\ &= 2s_0 \left(\tfrac{n_i}{n_e}\right)^2 \int_0^{\theta_{cie}} \sin\theta_i d\theta_i = 2s_0 \left(\tfrac{n_i}{n_e}\right)^2 [1 - \cos\theta_{cie}]. \end{aligned} \tag{96}$$

This expression is identical to that obtained with the other method (Eq. (42)).

## References


[1] Duderstadt JJ, Martin WR. Transport theory. New York: John Wiley and Sons; 1979.
[2] Martelli F, Bianco SD, Ismaelli A, Zaccanti G. Light propagation through biological tissue and other diffusive media: theory, solutions, and software. Bellingham: SPIE press; 2009.
[3] Paasschens JCJ. Solution of the time-dependent Boltzmann equation. Phys Rev E 1997;56:1135–41.
[4] Markel VA. Modified spherical harmonics method for solving the radiative transport equation. Wave Random Media 2004;14:L13–19.
[5] Panasyuk G, Schotland JC, Markel VA. Radiative transport equation in rotated reference frames. J Phys A 2006;39:115–37.
[6] Liemert A, Kienle A. Analytical Green's function of the radiative transfer radiance for the infinite medium. Phys Rev E 2011;83:036605–1–036605–7.
[7] Liemert A, Kienle A. Light transport in three-dimensional semi-infinite scattering media. J Opt Soc Am A 2012;29:1475–81.
[8] Liemert A, Kienle A. Exact and efficient solution of the radiative transport equation for the semi-infinite medium. Sci Rep 2013;3:2018–1–2018–7.
[9] Liemert A, Reitzle D, Kienle A. Analytical solutions of the radiative transport equation for turbid and fluorescent layered media. Sci Rep 2017;7:3819–1–3819–9.
[10] Machida M, Panasyuk GY, Schotland JC, Markel VA. The greens function for the radiative transport equation in the slab geometry. J Phys A 2010;43:065402–1–065402–2.
[11] Machida M. Singular eigenfunctions for the three-dimensional radiative transport equation. J Opt Soc Am A 2014;31:67–74.
[12] Machida M. How to construct three-dimensional transport theory using rotated reference frames. J Comput Theor Transp 2016;45:594–609.
[13] Machida M. The Green's function for the three-dimensional linear Boltzmann equation via fourier transform. J Phys A 2016;49:175001–1–175001–16.
[14] Bardsley J, Dubi A. The average transport path length in scattering media. SIAM J Appl Math 1981;40:71–7.
[15] Blanco S, Fournier R. An invariance property of diffusive random walks. Europhys Lett 2003;61:168–73.
[16] Mazzolo A. Properties of diffusive random walks in bounded domains. EPL 2004;68(3):350–5.
[17] Zoia A, Dumonteil E, Mazzolo A. Properties of branching exponential flights in bounded domains. EPL 2012;100(4):40002.
[18] de Mulatier C, Mazzolo A, Zoia A. Universal properties of branching random walks in confined geometries. EPL 2014;107(3):30001.
[19] Pierrat R, Ambichl P, Gigan S, Haber A, Carminati R, Rotter S. Invariance property of wave scattering through disordered media. PNAS 2014;111:17765–70.
[20] Tommasi F, Fini L, Martelli F, Cavalieri S. Invariance property in scattering media and absorption. Opt Commun 2020;458:124786.
[21] Savo R, Pierrat R, Najar U, Carminati R, Rotter S, Gigan S. Observation of mean path length invariance in light-scattering media. Science 2017;358(6364):765–8.
[22] Zoia A, Larmier C, Mancusi D. Cauchy formulas for linear transport in random media. EPL 2019;127(2):20006.
[23] Tommasi F, Fini L, Martelli F, Cavalieri S. Invariance property in inhomogeneous scattering media with refractive index mismatch. Phys Rev A 2020;102.043501–1–043501–7
[24] Dirac PAM. Approximate rate of neutron multiplication for a solid of arbitrary shape and uniform density. British Report MS-D-5; 1943. Part I
[25] Frangipane G, Vizsnyiczai G, Maggi C, Savo R, Sciortino A, Gigan S, Leonardo RD. Invariance properties of bacterial random walks in complex structures. Nat Commun 2019;10:2442.
[26] Case KM, Zweifel PF. Linear transport theory. London: Addison-Wesley Publishing Company, Massachusetts, Palo Alto; 1967.
[27] Tsuchiya Y. Photon path distribution and optical responses of turbid media: theoretical analysis based on the microscopic Beer-Lambert law. Phys Med Biol 2001;46:2067.
[28] Yablonovitch E. Statistical ray optics. J Opt Soc Am 1982;72:899–907.
[29] Lazutkin VF. The existence of caustics for a billiard problem in a convex domain. Math USSR Izv 1973;7:185–214.
[30] Majic M, Somerville WRC, Le-Ru EC. Mean path length inside nonscattering refractive objects. Phys Rev A 2021;103:L031502.
[31] Giovanelli RG. Reflection by semi-infinite diffusers. Opt Acta 1955;2:153–62.
[32] Hulst HCVD. Multiple light scattering. New York (USA): Academic Press; 1980.
[33] Martelli F, Contini D, Taddeucci A, Zaccanti G. Photon migration through a turbid slab described by a model based on diffusion approximation. II. Comparison with monte carlo results. Appl Opt 1997;36(19):4600–12.
[34] Barthelemy P, Bertolotti J, Wiersma DS. A Lévy flight for light. Nature 2008;453:459.